Characterization of RNA Granules in Muscle Stem Cells through TACC3 and DDX6

Harry Chun Man CHENG

Department of Human Genetics

Faculty of Medicine and Health Sciences

McGill University, Montreal

Submitted July 2022

A thesis submitted to McGill University in partial fulfillment of the requirements of the degree of Master of Science

Abstract

Muscle stem cells (MuSCs) are typically in a quiescent state and activate during muscle regeneration to allow the formation of new myofibers. Studies focusing on translational control have demonstrated the presence of messenger ribonucleoprotein (mRNP) granules in quiescent MuSCs and the dissolution of such granules during early activation to release mRNA transcript for rapid translation of myogenic factor. Some mRNAs can be sequestered by mRNP components such as DDX6 in the mRNP granules, potentially playing an important role in translational control during the establishment of quiescence and muscle regeneration. However, little is known about how the dynamics of these granules are regulated and how the granules change. Growing evidence suggests the dynamics of mRNP granules are regulated by the cytoskeletal structures such as microtubules. Given Transforming Acidic Coiled-Coil Containing Protein 3 (TACC3) has been reported to shift the microtubule dynamics and cargo transport in neuroblastoma and get selectively translated in a P-eIF2α dependent manner in muscle stem cells, I examined whether TACC3 is involved in the regulation of microtubule dynamics and hence the mRNP granules dynamics in MuSCs. Next, I examined how the mRNP granules change during the postnatal growth and myogenic program and the role of the mRNP granule component, DDX6, in MuSCs. Here, I examined the role of TACC3 in microtubule dynamics and muscle stem cell quiescence. However, the knockout of TACC3 did not shift the dynamic microtubule network to a stable de-tyrosinated microtubule network and had no observable phenotype on the MuSCs quiescence. Next, I focused on the changes in the number of granules and granule types during postnatal growth and myogenic program. The overall changes in the number of granules during postnatal growth were insignificant, in part due to the heterogeneity present. However, a significantly higher number of granules was observed in PAX7 (+) MYOD (+) cells compared to PAX7 (+) MYOD (-) cells on postnatal day 28. Similarly, during quiescent

MuSCs activation, a significant increase in the number of granules was observed in satellite cells cultured for 24 hours compared to 6 hours of culture. A significant increase in the fraction of P-bodies was also observed during satellite cells activation, alongside with upregulation of DCP1a. Lastly, knockdown of DDX6 in satellite cells was shown to cause premature differentiation. Overall, the results suggest mRNP granule may regulate the establishment of quiescence and muscle regeneration.

Résumé

Les cellules souches musculaires (MuSCs) existent normalement en état de quiescence et deviennent activées lors de la régénération musculaire afin de former de nouvelles fibres musculaires. Plusieurs études portant sur la régulation via la traduction ont souligné la présence de granules de « messenger ribonucleoprotein » (mRNP) dans les MuSCs et notent que celles-ci se dissolves lors de l'activation des MuSCs, libérant l'ARN et permettant la traduction rapide des facteurs myogéniques. Certains mRNA peuvent être séquestrés par des composants mRNP tels que DDX6 dans les granules mRNP. Ceci joue potentiellement un rôle important dans le contrôle traductionnel lors de l'établissement de la quiescence et la régénération musculaire. Cependant, nous en savons peu sur comment la dynamique de ces granules est régulée ainsi que sur la façon dont ces granules changent. Un nombre croissant d'études suggère que la dynamique des granules de mRNP est régulée par les structures du cytosquelette telles que les microtubules. Étant donné qu'il a été rapporté que la protéine « Transforming Acidic Coiled-Coil Containing Protein 3 » (TACC3) modifie la dynamique des microtubules et le transport dans les neuroblastomes et qu'elle est traduite sélectivement de manière dépendante de P-eIF2α dans les cellules souches musculaires, j'ai examiné si TACC3 est impliquée dans la régulation de la dynamique des microtubules ainsi que dans la dynamique des granules mRNP dans les cellules souches musculaires. J'ai ensuite examiné comment les granules mRNP changent au cours de la croissance postnatale ainsi que lors du programme myogénique. J'ai aussi examiné le rôle du composant des granules mRNP, DDX6, dans les cellules souches musculaires. Ici, j'ai étudié le rôle de TACC3 dans la dynamique des microtubules et la quiescence des cellules souches musculaires. Le knock-out de la TACC3 ne pousse pas le système dynamique de microtubules vers un système de microtubules détyrosiné et stable. De plus, ce knock-out n'a pas d'effet visible sure la quiescence des MuSCs. Je me suis ensuite concentré sur les variations de nombres de

granules ainsi que types de granules lors de la croissance post-natale et du programme myogénique. Les variations de nombres de granules lors de la croissance post-natale étaient non-significatives, en partie dû à l'hétérogénéité de ces cellules. Pourtant un nombre significativement élevé de ces granules fût observé dans les cellules PAX7 (+) MYOD (+) par rapport aux cellules PAX7 (+) MYOD (-) au jour post-natal 28. De plus, lors de l'activation des MuSCs quiescentes, une augmentation significative de granules fût observée dans les MuSCs en culture pour 24 heures versus celles en culture pour 6 heures. Une augmentation significative dans la proportion de « P-bodies » fut aussi observée lors de l'activation des MuSCs, accompagné par l'augmentation de DCP1a. Finalement, le knock-down de DDX6 dans les MuSCs a entrainé la différentiation prématurée de ces cellules. Globalement, les résultats suggèrent que le granule mRNP peut réguler l'établissement de la quiescence et la régénération musculaire.

Table of Contents

List of Abbreviations

APEX: Ascorbate peroxidase

b-isox: Biotinylated isoxazole

BrdU: Bromodeoxyuridine

CAV1: Caveolin 1

CPEB: Cytoplasmic polyadenylation element binding protein

DCP1A: mRNA-decapping enzyme 1A

DDX6: DEAD-Box Helicase 6

Dll1: Delta Like Canonical Notch Ligand 1

Dpi: Days post-injury

eIF: Eukaryotic translation initiation factor

FACS: Fluorescence-activated cell sorting

FAP: Fibro-adipogenic progenitor

FAPS: Fluorescence-activated particle sorting

Fl: Floxed

FMRP: Fragile X mental retardation protein

FOXO: Forkhead box transcription factor class O

G3BP1: Ras GTPase-activating protein-binding protein 1

GCN2: general control non-derepressible-2

HRI: heme-regulated inhibitor

KDM4B: Lysine-specific demethylase 4B

LC: Low complexity

microRNA: miRNA

miRISC: miRNA-induced silencing complex

mRNA: Messenger RNA

mRNP: Messenger ribonucleoprotein

MYOG: Myogenin

P-bodies: Processing bodies

PERK: protein kinase RNA-like endoplasmic reticulum kinase

PKR: double-stranded RNA

PTM: Post-translational modification

RBP: RNA binding proteins

sc-RNA-seq: single cell RNA-seq

Sdc4: Syndecan 4

smFISH: single molecule fluorescence in situ hybridization

SUMO: Small ubiquitin-like modifier

TACC3: Transforming Acidic Coiled-Coil Containing Protein 3

TCDD: 2,3,7,8-tetrachlorodibenzo-p-dioxin

uORF: upstream open reading frame

UTR: Untranslated region

VCAM1: Vascular Cell Adhesion Molecule 1

WISP1: WNT1 Inducible Signaling Pathway Protein 1

List of Figures

Acknowledgements

I would like to thank my supervisor, Dr. Colin Crist for the opportunity to work in his lab and for all the support and advice throughout my master's studies.

I would also like to thank the members of my supervisory committee, Dr. Carl Ernst and Dr. Thomas Durcan for the advice during the meetings.

I would like to thank my colleague, Ms. Solène Jamet for providing me with advice and help in my experiments and Ms. Charlotte Sénéchal for translating the abstract into French.

I would like to thank Christian Young and particularly Mathew Duguay for all the cell sorting we have done and the support in the imaging facility.

Thank you to Mr. Li Chun Hei for the support and criticism on my research.

Thank you to Regan and Hugo for the support during my graduate studies.

Thank you to Hamlet, who I will be forever grateful.

Lastly, I would like to thank my family, especially my mum, in Hong Kong for supporting my graduate studies during this difficult COVID time.

Format of the Thesis

The thesis is presented in the format of a traditional thesis according to the guidelines stated by the Graduate and Postdoctoral Studies at McGill University.

Contribution of Authors

The work presented in this thesis was designed by Dr. Colin Crist and I. I performed and analyzed all the experiments performed. Charlotte Sénéchal translated of the abstract of this thesis into French. Christian Young and Mathew Duguay assisted with FACS.

Chapter 1: Introduction

Stem cells are undifferentiated cells that can differentiate into different cell types to form tissues and organs in our body and replace cells when needed. They are able to self-renew, generate new cells, and differentiate to replenish dead or damaged cells. During the regeneration process or aging, some of these stem cells are lost. The need of our body to replenish cells through stem cells drives the study of somatic stem cells to understand their properties and strategize therapies against diseases and aging.

1.1. Satellite Cells

Adult muscle stem cell, also called satellite cell, is one of the types of somatic stem cell found in muscles. They are poised in a quiescent state and activate rapidly upon injury to regenerate the muscle tissue.

1.1.1. Discovery of satellite cell

Satellite cell was named after its satellite position around the muscle fiber. It was first reported in skeletal muscle fiber in the peripheral region using electron microscope in 1961 (Mauro, 1961). Later studies showed that satellite cells undergo mitosis (Moss and Leblond, 1970; Reznik, 1969) and are responsible for muscle regeneration (Schmalbruch, 1976), suggesting their role as stem cells.

Through in situ hybridization, PAX7 was later identified as one of the characteristic markers for satellite cells (Seale et al., 2000), which is now commonly used to identify quiescent satellite cells. Other than PAX7, a majority of the PAX7 expressing cells in the trunk muscles, such as diaphragm, co-expresses PAX3 (Relaix et al., 2006). Therefore, PAX3 was also used in some protocols to isolate quiescent satellite cells (Montarras et al., 2005).

1.1.2. Quiescence

Quiescent state is a reversible cell cycle arrest. Satellite cells are usually quiescent at rest but can rapidly re-enter the cell cycle in response to injury or changes in the satellite cell niche. Some of the characteristics of quiescent satellite cells include a high nucleus-to-cytoplasm ratio (LaBarge and Blau, 2014), low metabolic rate (Chen et al., 2020), and lower transcription (Massenet et al., 2021). Study of the satellite cell quiescence reveals the importance of activation of Notch signalling pathway in maintaining the quiescence while activation of other pathways such as Wnt pathway and mTORC signaling are important in the quiescence exit (Zhou et al., 2022). During quiescence, satellite cells express Notch1-3 and Notch targets are sharply downregulated after injury (Mourikis et al., 2012). Binding of Dll1 to Notch receptors causes translocation of NICD to the nucleus and upregulation of quiescent genes, such as the Hes/Hey family (Bjornson et al., 2012). Moreover, NICD was also shown to regulate the *Pax7* through interaction with RBP-Jκ and binding to the 5' region of the *Pax7* gene (Wen et al., 2012). In addition to Notch, FoxO transcription factors are also highly expressed during quiescence (García-Prat et al., 2020). Interestingly, ablation of FoxO3 only in satellite cells has no obvious phenotype or loss of satellite cell quiescence but impaired satellite cell self-renewal (Gopinath et al., 2014), and ablation of FoxO1 only resulted in a similar phenotype (García-Prat et al., 2020). However, triple-mutant of FoxO1, FoxO3a, and FoxO4 resulted in spontaneous activation and differentiation of satellite cells (García-Prat et al., 2020), suggesting functional redundancy and importance of the FoxO family. In relation to Notch signaling, FoxO3 was also shown to regulate Notch1 and Notch3 expression (Gopinath et al., 2014). Other signaling pathways, such as calcitonin receptor (CalcR) signaling, mediate quiescence maintenance through inhibiting activation of pathways required in satellite cell activation and proliferation. For example, CalcR signaling was reported to maintain the quiescence of satellite cells by inhibiting Hippo signaling, which

regulates cell proliferation (Zhang et al., 2019).

Besides the quiescent state during the resting phase (G_0), satellite cells can also enter an alert phase called G_{alert} (Rodgers et al., 2014). The discovery of G_{alert} phase was through studying distant injury in the mouse model (Rodgers et al., 2014). In injured mice, satellite cells from the uninjured muscle showed an increase in cell size and accelerated cell cycle entry (Rodgers et al., 2014). The G_{alert} phase was shown to be mediated through activation of mTORC1 signaling via the hepatocyte growth factor (HGF) receptor, cMet (Rodgers et al., 2014). The transcriptional profile of the alert state can be reversed 28 days post-injury (dpi) (Rodgers et al., 2014). Satellite cells in the G_{alert} phase allow a rapid response under stress conditions while remaining in a quiescent state (Rodgers et al., 2014). mTORC1 signaling also plays a role in translational control, which will be further discussed in Chapter 1.2.

Overall, the quiescence is suggested to be important in maintaining a long-term capacity to regenerate the muscle and replenish the satellite cells pool when needed (Ancel et al., 2021).

1.1.3. Postnatal growth

Before the MuSCs establish quiescence, the myogenic progenitors undergo expansion and differentiation to allow muscle growth after birth until reaching adulthood. During the postnatal growth, the composition of different myogenic populations changes and heterogeneity was observed (Gattazzo et al., 2020). In the early postnatal growth of muscle, the myogenic progenitors mainly undergo expansion to further increase the PAX7 (+) cells pool (Gattazzo et al., 2020). Increase in the commitment of myogenic progenitors, PAX7 (-) MYOD (+) cells, was observed from postnatal day 5 to 6 and 15 to 21 (Gattazzo et al., 2020). Two waves of increase in myogenic differentiation were followed respectively, from postnatal day 7 to 10 and 21 to 28 (Gattazzo et al., 2020). The sub-laminal position of the

myogenic progenitors was not fully developed until postnatal day 28, along with a significant increase in quiescent myogenic progenitors (Gattazzo et al., 2020). Through KI67 staining, it was also demonstrated that the establishment of quiescence in myogenic progenitors was not fully completed until between postnatal day 49 and 56 (Gattazzo et al., 2020).

Interestingly, the myogenic cells at different stages of development behave differently, ranging from their shape, response to molecules (Biressi et al., 2007), and ability to differentiate (Tierney et al., 2016). Single-cell RNA-seq also confirmed the PAX7(+) myogenic progenitors are not identical during development (Xi et al., 2020). So far, it is still not fully understood how the myogenic progenitors transition from proliferation to quiescence during postnatal growth and, why and how the proliferating myoblast during postnatal growth differ from adult proliferating myoblast.

1.1.4. Satellite cell niche

After the satellite cells establish quiescence in adulthood, their microenvironment, which is also called niche, plays a crucial role in maintaining the quiescence and regeneration of satellite cells. Interestingly, satellite cells act autonomously to maintain their niche during quiescent state. Collagen V is produced by satellite cells as one of the components in the niche and loss of collagen V led to cell cycle entry (Baghdadi et al., 2018). Notch signaling was also suggested to be a sensor for collagen V production, given the presence of NOTCH/RBPJ-bound regulatory elements adjacent to collagen genes (Baghdadi et al., 2018), and control adhesion to myofibers (Bröhl et al., 2012). Collagen V interacts with satellite cells through CalcR, however, the downstream signalling remains to be studied (Baghdadi et al., 2018). Upon disruption of the niche, collagen V production decreases with notch signaling downregulation to favor activation, forming a positive feedback loop (Baghdadi et al., 2018). Another example is the secretion of vascular endothelial growth factor A(VEGFA)

to attract endothelial cells, which express Dll4 to maintain satellite cell quiescence (Verma et al., 2018). Deletion of VEGFA in satellite cells led to reduction in proximity to capillaries and affect satellite cells self-renewal (Verma et al., 2018). Besides the satellite cells, the surrounding environment, such as myofiber, also plays a role. Myofibers secrete Wnt4 to activate Rho satellite cells to maintain satellite cell quiescence and repress Yap expression (Eliazer et al., 2019), which is upregulated during activation (Judson et al., 2012). Other cell types in the niche can also interact with satellite cells. Macrophages infiltrate during muscle injury and release glutamine to activate mTORC and promote muscle regeneration (Shang et al., 2020). Fibro-adipogenic progenitors (FAP) secrete WISP1, which controls satellite cell expansion and asymmetric cell division through Akt signaling (Lukjanenko et al., 2019). Given the complexity of the satellite cell niche, with participation from different cell types, *in vitro* culture system may not be able to fully recapitulate *in vivo* regeneration very well and hence, causing a discrepancy in observation in the myogenic program.

1.1.5. Regeneration

Upon muscle injury or disruption in homeostasis in satellite cell niche, quiescent satellite cells get activated (Figure 1). Satellite cells start expressing myogenic factors such as MYF5 and MYOD (Cornelison and Wold, 1997). The activated satellite cells undergo proliferation to increase cell numbers. Some will continue to downregulate PAX7 and start expressing MYOGENIN and differentiate (Olguin and Olwin, 2004). Upregulation of muscle-specific membrane proteins, MYOMIXER and MYOMAKER, then allows cell fusion and hence, muscle regeneration (Bi et al., 2018; Millay et al., 2014). While many activated satellite cells will contribute to the regeneration process, some will downregulate myogenic factors, such as MYOD, for self-renewal instead of proceeding to differentiation (Zammit et al., 2004)

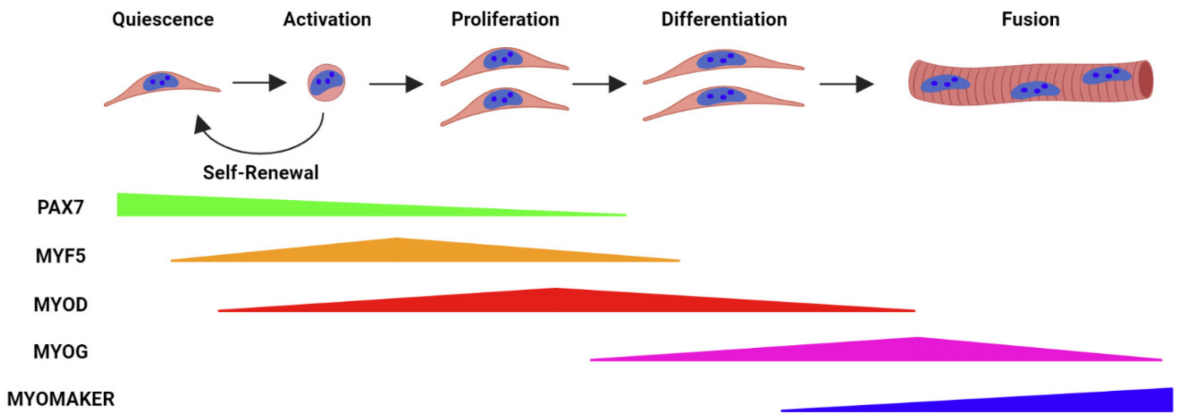

Figure 1. Illustration of myogenic program in satellite cells.

1.1.6. Self-renewal

During muscle regeneration, some muscle stem cells self-renewal to maintain the MuSC pool and prevent exhaustion. In earlier study, the self-renewal property in satellite cells was reported in BrdU labeling experiments where a population of daughter cells did not get labeled, suggesting they may have gone through asymmetric division to generate myogenic progenitors for fusion (Schultz, 1996). Two mechanisms have been proposed to regulate satellite cell self-renewal: asymmetric cell division and symmetric cell division. Asymmetric cell division generates one daughter cell retaining the stemness and another daughter cell committed to differentiation while symmetric cell division generates two daughter cells both retaining the stemness and one of them later becomes committed to differentiation. Several studies have been favoring the concept of asymmetric cell division. One of the myogenic factors, MYF5, exhibits asymmetric division in cultured myofibers (Kuang et al., 2007). Using a *Myf5*^{Cre}*; ROSA26*^{YFP} reporter mice, PAX7^{+}/MYFf5^{-} satellite cells were found to undergo asymmetric cell division through apical-basal oriented cell division, generating a basal PAX7^{+}/MYF5^{-} and an apical PAX7^{+}/MYF5^{+} cells (Kuang et al., 2007). Such apical-basal oriented cell division was shown to be mediated through polarization of dystrophin, which associates with the serine-threonine kinase Mark2 to

regulate cell polarity by localizing Pard3 to the cell periphery (Dumont et al., 2015). Another protein important in the commitment of satellite cells, Numb, was also found to be localized asymmetrically during cell division (Conboy and Rando, 2002). In a recent study, intracellular organelle, lipid droplets (LD), are also found to be distributed asymmetrically during cell division, with LD^{Low} cells tending to self-renewal while LD^{High} cells tending to differentiate (Yue et al., 2022). In other stem cells, other organelles, such as mitochondria, have also been suggested to have selective inheritance in daughter cells, potentially providing a metabolic bias for cell fate decisions (Döhla et al, 2022). Altogether, it indeed suggests satellite cells undergo asymmetric cell division. However, it remains elusive whether the asymmetric localization of different proteins and organelles is a cause or consequence. Some studies suggest that asymmetric cell division is mediated by the satellite cell niche. By manipulating the extracellular matrix through micropatterning, non-random DNA segregation and asymmetric cell fate were also observed (Yennek et al., 2014). However, single-cell tracking over multiple cell division is lacking to address whether the cell fate is determined over time or simply through one asymmetric cell division.

A recent study reveals that self-renewal of MuSCs mostly takes place during the timeframe from 5 dpi to 7dpi, with some taking place between 2dpi and 4dpi (Cutler et al., 2021), suggesting the adoption of symmetric cell division in the early stage of regeneration. Moreover, transplantation of MuSCs into freshly injured muscle versus 5dpi muscle showed a difference in cell fate decision and hence the effect of environmental cues in MuSC fate determination (Cutler et al., 2021). A similar switch from symmetric cell division to asymmetric cell division was also observed between 3 dpi and 5dpi using H3 SNAP labelling (Evano et al., 2020). The difference observed in reported studies (Feige et al., 2018; Kuang et al., 2007; Troy et al., 2012) may be in part explained by the model of study focusing on

isolated myofibers, which lack signaling cues from the niche. Further *in vivo* tracking may be required to further understand muscle stem cell self-renewal.

1.1.7. Heterogeneity of satellite cells

Through studies of different aspects of satellite cells, one important characteristic of satellite cells has been observed: heterogeneity. Heterogeneity in satellite cells has been described in several studies, however, it remains unclear what mechanism regulates the heterogeneity and how it impacts studies of muscle regeneration and self-renewal. In earlier clonal studies, heterogeneity in satellite cells was observed in individual satellite cells (Siegel et al., 2011), muscles (Lagord et al., 1998), developmental origins (Ono et al., 2011). Further studies in the heterogeneity revealed mechanisms behind the cell fate decision between self-renewal and differentiation. In the immortal DNA strand hypothesis (Cairns, 1975), it was hypothesized the stem cell pool minimizes accumulation of replication-induced mutations by asymmetric cell division. Aligned with the hypothesis, $PAX7^{High}$ satellite cell was described to have distinct asymmetric segregation of DNA template (Rocheteau et al., 2012). The ability of the $PAX7^{high}$ population to replenish itself after transplantation suggested there may be a stem cell hierarchy present in the muscle satellite cells (Rocheteau et al., 2012). In the functional aspect, a rare subpopulation co-expressing PAX3 was found in the satellite cells (Der Vartanian et al., 2019, Scaramozza et al., 2019). The population showed reserve stem cell properties and exhibited resistance to environmental stress such as TCDD, a highly toxic pollutant (Der Vartanian et al., 2019), and radiation stress (Scaramozza et al., 2019), suggesting the heterogeneity does have functional implications. Studies to look at whether the heterogeneity is intrinsic were also performed. Using a lineage tracing model, a subpopulation of adult satellite cells has never expressed MYF5 during development and has a higher contribution to self-renewal (Kuang et al., 2007). The phenomenon was further supported by the study where MYF5 protein was shown to be expressed in the majority of

satellite cells and haploinsufficiency in MYF5 resulted in higher self-renewal capacity than wild-type cells (Gayraud-Morel et al., 2012). With the recent advances in sc-RNA-seq, subpopulations in satellite cells were further supported. In one study, two subpopulations were described, one depleted in *Myf5* expression and one enriched in *Sdc4* and *Notch2* (Yartseva et al., 2020). In human data, single-cell RNA-sequencing also revealed heterogeneity. A subpopulation of human MuSCs expressing CAV1 was more resistant to activation and demonstrated better engraftment than CAV1(-) cells (Barruet et al., 2020).

The heterogeneity in different studies consistently demonstrated the difference in the ability to self-renewal and differentiate. However, the current studies in heterogeneity focus on genomics. Although functional validations were performed to identify the populations, it remains unclear how satellite cells differ in proteomics. With the advances in sc-Mass Spectrometry, it may shed light on the heterogeneity among satellite cells and help understand how the cell fate decision is regulated.

1.2. Translational Control

Different levels of control are used to regulate the protein level, from transcription to translation and degradation. During satellite cell activation, rapid response is observed, and translational control may allow cells to achieve such purpose. Therefore, in this study, I focused on the regulation of gene expression by translational control.

1.2.1. mRNA life cycle

RNA metabolism is the molecular process that determines the RNA fate, from synthesis to degradation. RNA binding proteins form messenger ribonucleoprotein with the mRNA during the mRNA life cycle to regulate the process. The life cycle of mRNA starts from transcription in the nucleus. The newly synthesized pre-mRNA undergoes different maturation processes including the addition of 5’ cap, polyadenylation at the 3’ end, and pre-

mRNA splicing. Mature mRNA will be exported from the nucleus to the cytoplasm. Some mRNA will undergo translation to yield the protein and some mRNP will assemble into mRNP granules for storage or degradation. The storage of repressed mRNA will be further discussed in Chapter 1.3. To degrade the mRNA, most transcripts undergo deadenylation by the PAN2-PAN3 complex and CAF1-CCR4-NOT complex, followed by either degradation in exosome or decapping by DCP family and exonucleolytic degradation (Coppin et al., 2018). The translation of mRNA is regulated by different mechanisms. Depending on the mechanism involved, it can impact the global translation and/or translation of specific mRNA.

1.2.2. Global control of translation

Global control of translation is mainly mediated by translation-initiation factors and their phosphorylation states. One of the initiation factors is eIF2. During translation initiation, the GTP bound to the eIF2 is hydrolyzed and the exchange of GDP for GTP is required for another round of translation initiation. The GTP exchange is regulated by the phosphorylation of the α subunit of eIF2 at the amino acid residue Ser51 by forming an eIF2αP/eIF2B inhibitory complex (Adomavicius et al, 2019). Four different kinases are identified to regulate the eIF2α phosphorylation, including protein kinase activated by double-stranded RNA (PKR), protein kinase RNA-like endoplasmic reticulum kinase (PERK), heme-regulated inhibitor (HRI), and general control non-derepressible-2 (GCN2). The phosphorylation of eIF2α is induced by different kinases under different conditions. PKR is induced in response to viral infection to reduce translation of viral mRNA and promote apoptosis. PERK is induced during endoplasmic reticulum stress to allow time for refolding misfolded protein. HRI is induced when the heme levels are low in the cell. GCN2 is induced in response to nutrient deprivation, such as amino acids and glucose.

Though overall, the translation is repressed, some transcripts with upstream open reading frames (uORF) get selectively translated (Young and Wek, 2016). For example, during the cellular stress with an increased P-eIF2α level, the level of eIF2-GTP is lowered and delays the acquisition of eIF2 ternary complex in the inhibitory uORF of *Atf4* and hence, allows the initiation at *Atf4* coding sequence (Young and Wek, 2016). The preferential translation of *Atf4* regulates the gene expression of stress-responsive genes and such response is commonly known as the integrated stress response (Young and Wek, 2016). GADD34, which promotes the dephosphorylation of eIF2α, also has uORFs and the transcription of *Gadd34* is upregulated by ATF4 to regulate translation repression (Donnelly et al., 2013). As a negative feedback loop, GADD34 can bind with PP1 to form a phosphatase complex that allows the dephosphorylation of eIF2α to restore protein synthesis (Young and Wek, 2016).

Another global translational control is the regulation of the availability of eIF4E. During translation initiation, the recruitment of the 43S ribosomal complex is mediated by the interaction between eIF4E and eIF4G (Amorim et al., 2018). The availability of eIF4E is regulated by 4E-binding protein (4E-BP). Hypo-phosphorylated 4E-BP displaces eIF4G and hence prevents the association between eIF4E and eIF4G and represses translation initiation (Amorim et al., 2018). Phosphorylation of 4E-BP is regulated by mTOR signaling and hence allows the regulation of eIF4E and translation (Koromilas et al., 2019). During stress, increased P-eIF2α level inhibits mTORC1 through upregulation of SENS2 and REDD1 (Koromilas et al., 2019). Phosphorylation of 4E-BP by mTORC1 is therefore inhibited and the availability of eIF4E decreases. When cellular stress is lifted, the phosphorylation of 4E-BP by mTORc1 allows the eIF4E to bind to eIF4G again and resume translation (Koromilas et al., 2019). eIF4E is also identified in mRNP granules, along with 4E-BP (Andrei et al., 2005). The re-localization of eIF4E to mRNP granules may further aid in the translation repression.

1.2.3. mRNA-specific translation control

Contrary to the global translation control, mRNA-specific translational control is the regulation of translation of a specific type of mRNA without changing the overall protein synthesis. One such control is mediated by microRNA (miRNA). miRNA is the small regulatory RNA that allows translation control of specific mRNA (O'Brien et al., 2018). miRNA acts by incomplete hybridization to the target mRNA, usually at the 3' UTR (O'Brien et al., 2018). miRNA-mediated gene silencing was achieved through miRNA-induced silencing complex (miRISC), which contains proteins such as the AGO family and GW182 family (O'Brien et al., 2018). The degree of complementary sequence between the microRNA and the target mRNA sequence determines whether the mRNA gets silenced or degraded (O'Brien et al., 2018). The incomplete hybridization prevents degradation by the AGO2 endonuclease (O'Brien et al., 2018). It is, however, unclear whether the miRISC requires structures such as mRNP granules for its action. miRNA and components of the miRISC have been reported to colocalize to mRNP granules (O'Brien et al., 2018). Hence, it has been suggested that miRISC is shuttled to mRNP granules for storage and degradation.

Different RNA binding proteins have been reported to be involved in reversing the miRNA-mediated gene silencing. For example, phosphorylation of FMRP was shown to promote the formation of AGO2 inhibitory complex while dephosphorylation promotes the release of AGO2 from the mRNA (Muddashetty et al., 2011). A similar observation was reported in satellite cells where phospho-FMRP is present during quiescent state and FMRP dephosphorylates upon activation, in concomitant with the accumulation of MYF5 protein, which is repressed by microRNA-31 (Crist et al., 2012).

1.2.4. RNA binding protein

Both global and mRNA-specific control of translation require RNA binding proteins (RBP). They are involved in the formation of mRNP granules through binding with RNA. RBP binds to RNA via RNA-binding domains such as RNA recognition motif, hnRNP K homology domain, or DEAD-box helicase domain (Hentze et al., 2018). The RBP can bind to the RNA to regulate the fate of the mRNA and alternatively, RNA, such as long non-coding RNA, can bind to RBP to regulate the fate of the RBP (Hentze et al., 2018). RNA binding sites were also found to be enriched in post-translational modification sites such as acetylation and phosphorylation, suggesting a potential mechanism to regulate binding and function (Castello et al., 2016). Different modes of regulation were shown for RBP. RBP can have high-specificity binding to target-specific mRNA for processing, localization, or translation (Hentze et al., 2018). On the other hand, RBP can have low specificity binding such as translation initiation factors during the translation initiation process (Hentze et al., 2018). RBP can also modulate its functions through binding with RNA, for example, binding of PKR to viral dsRNA allows dimerization of PKR and autophosphorylation of PKR to activate PKR and allow subsequent phosphorylation of eIF2α to block protein synthesis (Balachandran et al., 2007). RBP also plays an important role in the formation of mRNP granules and translation repression, which will be further discussed in chapter 1.3. The diverse role of RBP allows cells to regulate different cellular processes. It has also been proposed that the localization of RBP may provide a potential mechanism to regulate their function. It can allow rapid response in the cell without the need for transcription or translation, which makes studies of mRNP granules an interesting topic.

1.2.5. Translation control in satellite cell

Translational control has also been studied in satellite cells. In quiescent satellite cells, the quiescence state was shown to be maintained by global translation repression through PERK phosphorylation of eIF2α (Zismanov et al., 2016). Genes with uORFs, such as Atf4 and Chop, were selectively translated in quiescent satellite cells compared to activated satellite cells after 3 days of culture, in concomitant to the drop in P-eIF2α level (Zismanov et al., 2016). Mutation in the phosphorylation site S51 to alanine in conditional knockout satellite cells caused quiescence exit and mRNP granules disassemble (Zismanov et al., 2016), suggesting the importance of P-eIF2α in quiescence maintenance. *Ex vivo* culture using the eIF2α phosphatase inhibitor sal003 further showed the ability of freshly isolated satellite cells to maintain a high level of Pax7 and higher regenerative potential (Zismanov et al., 2016). By comparing the satellite cells cultured in sal003 and DMSO control through mass spectrometry and RNA-seq, a set of proteins was found to be upregulated independent of mRNA level (Fujita et al., 2021). One of the genes, *Tacc3*, was shown to have uORFs, which enable translation in the presence of sal003 (Fujita et al., 2021). Though the knockout of TACC3 did not impact the maintenance of quiescence in satellite cells (Fujita et al., 2021), the other genes with uORFs may be a potential level of translational control in satellite cells.

Other than global repression of translation, mRNA-specific translational control is present in satellite cells. Translation of different proteins has been shown to be repressed by microRNA and/or RNA binding proteins. Through miRNA expression profiling during satellite cell activation, *miR-489* has been identified to be enriched in quiescent state and inhibition of *miR-489* causes quiescence exit (Cheung et al., 2012). Further investigation identifies Dek as the target of *miR-489* (Cheung et al., 2012) and DEK protein is important in processing intron-retained transcripts in quiescent satellite cells, such as myogenic factor *Myod1* (Yue et al., 2020). Myogenic factor *Myf5* is another example of repression through

microRNA. During quiescent state, *miR-31* was shown to target *Myf5* mRNA and both were targeted by DDX6 (Crist et al., 2012). The sequestering of *Myf5* mRNA and *miR-31* in DDX6 mRNP granules regulates the translation of *Myf5* (Crist et al., 2012). Upon activation, MYF5 protein accumulates, in concomitant with the dissociation of mRNP granules and *miR-31* downregulation (Crist et al., 2012). The sequestration of mRNA in mRNP granules may potentially provide an early response during activation of satellite cells. Other RNA binding proteins may also have translation regulation. STAUFEN1 has been shown to bind to the secondary structure in the 3'UTR of *Myod* transcript and co-localization between *Myod* mRNA and STAUFEN1 was observed through single molecule fluorescence in situ hybridization (smFISH) (de Morrée et al., 2017). The function of STAUFEN1 is likely to be mediated by the RNase UPF1 to degrade transcript (de Morrée et al., 2017). Co-localization of *Myod* transcripts with an RNase UPF1 and knockdown of UPF1 rescued reduction of *Myod* transcript induced by STAUFEN1 (de Morrée et al., 2017). Interestingly, it was reported that STAUFEN1 did not colocalize with the DDX6 (de Morrée et al., 2017) while other papers suggested STAUFEN1 was recruited to mRNP granules during stress (Thomas et al., 2009). Studies of RNA binding proteins may allow us to further understand the translation regulation of different transcripts due to their ability to bind to RNA and some with a role in mRNP granules.

1.3. Messenger ribonucleoprotein granules

Messenger ribonucleoprotein granules (mRNP granules), also called RNA granules, can also act as a translational control, as described earlier. mRNPs are dynamic, non-membrane bound condensates formed from RNA-binding proteins and mRNA through liquid-liquid phase separation. Interaction between mRNA and RNA-binding proteins is ubiquitous in cells and results in the formation of ribonucleoprotein particles (Singh et al., 2015). These mRNP particles, in turn, form mRNP granules. One of the earliest examples of

the observation of liquid-like compartments was the germ granules, P granules, in *Caenorhabditis elegans* embryos observed through electron microscopy (Wolf et al., 1983). A variety of mRNP granules have also been discovered, such as P-bodies (Sheth and Parker, 2003), GW bodies (Eystathioy et al., 2002), and stress granules (Collier and Schlesinger, 1986). Different types of mRNP granules have been shown to be associated with post-transcriptional regulation (Tian et al., 2020). Such reversible compartmentalization of mRNA allows cells to respond rapidly when needed (Lai et al., 2020). The exact role of the mRNP granules in different cell types remains unclear.

1.3.1. Assembly and disassembly of granules

To assemble these mRNP granules, low-complexity sequences and RNA binding activities are suggested to be important in the formation (Luo et al., 2018). The idea of the role of low complexity sequence in the assembly of mRNP granules stemmed from the discovery of RNA-binding proteins precipitated by a chemical called biotinylated isoxazole (b-isox) with many being the constituents of mRNP granules (Kato et al., 2012). Such low complexity sequence was able to aggregate into hydrogel-like state (Kato et al., 2012) and recruit mRNA that was precipitated by the b-isox chemical (Han et al., 2012). Furthermore, LC sequences are found in different domains of RNA binding proteins in mRNP granules (Luo et al., 2018). Altogether suggests the LC sequence may be involved in mRNP granule assembly. However, mutagenesis studies also suggested phase separation depend on collective interactions with amino acid residues outside the LC sequence (Wang et al., 2018). It remains unclear how different sequences in the RNA-binding protein modulate the assembly of RNA granules. Recent studies using an *in vitro* approach with ArtiGranule (Garcia-Jove Navarro et al., 2019) may help us further understand the role of different sequences in RNA binding protein in the formation of different granules. Using genetic engineering, a structural interaction domain, F36M-FKBP, was inserted into an oligomeric

protein, FERRITIN (Garcia-Jove Navarro et al., 2019). The F36M-FKBP protein has a point mutation in Phe36 in the FK506-binding protein, allowing formation of homodimers with micromolar concentration (Garcia-Jove Navarro et al., 2019). The scaffold formed by this protein assembles into ArtiGranule when a certain concentration is reached (Garcia-Jove Navarro et al., 2019). It allows recapitulation of phase separated liquid condensates in living cells and hence allows the study of different RNA binding domains. The study using ArtiGranule revealed the role of mRNA in condensate nucleation and the recruitment of specific RNA-binding proteins by the presenting mRNA on the surface of the assemblies (Garcia-Jove Navarro et al., 2019). It could eventually help to understand what RNA-binding protein and sequence are indispensable for the formation of RNA granules.

Contrary to the assembly of mRNP granules, the disassembly is not as well-studied. Polyribosomes on the mRNA have been suggested to be one of the key factors in the equilibrium in assembly and disassembly of the granules. Drug treatments that prevent translation exit, such as cycloheximide, promote disassembly of mRNP granules (Brengues et al., 2005) while drug treatment that promotes translation termination, such as puromycin, promote assembly of mRNP granules (Kedersha et al., 2000). In addition, post-translational modifications such as phosphorylation of eIF2α were also suggested to be crucial in granules assembly and disassembly, given its role in translational arrest (Kedersha et al., 1999). The disassembly process in stress granules is proposed to be through multiple steps, with RNA first getting titrated out of the granules, followed by structural instability and disassembly into smaller core structures that are eventually cleared out (Wheeler et al., 2016). The mechanism regulating the disassembly remains elusive. A recent study does support the disassembly of granules may be regulated. A group of proteins named disassembly-engaged proteins is recruited during stress granules disassembly, including small ubiquitin-like modifier (SUMO) conjugating enzymes (Marmor-Kollet et al., 2020). It suggests

SUMOylation is involved in the control of stress granules disassembly rather than a passive dissolution (Marmor-Kollet et al., 2020). The mechanism of how SUMOylation mediates the disassembly of granules, however, requires further studies. It is also unknown whether the assembly and disassembly process is conserved in different types of mRNP granules.

1.3.2. mRNP granules and microtubule network

Related to the dynamics of the mRNP granules, another key aspect of mRNP granules is their transport through cytoskeletal structures. mRNP granules, such as P-bodies, are localized to the cytoskeleton and move along the microtubules directionally (Aizer et al., 2008). Indeed, some studies have shown directed transport to deliver mRNA in neuronal synapses (Dalla Costa et al., 2020) and myofiber (Denes et al., 2021) through microtubules. Translation of some transcripts is also reversibly controlled by the microtubule dynamics (Carbonaro et al., 2011). In agreement with the observation of mRNP granules transport, mass spectrometry data in immunoprecipitation experiments using P-bodies components such as DDX6 (Di Stefano et al., 2019) and in P-bodies isolated with FAPS (Hubstenberger et al., 2017) identified several microtubule subunits and myosin motor families. Functional validation using dominant-negative tail construct of the motor protein showed decoupling of P-bodies from the microtubule (Lindsay and McCaffrey, 2011). Different studies also showed the role of motor proteins such as MyoVa, dynein, and kinesin in regulating the assembly and disassembly of P-bodies and stress granules (Lindsay and McCaffrey, 2011, Loschi et al., 2009). Altogether suggests the association of mRNP granules with the cytoskeleton and the potential regulation of translation through microtubules. However, it remains unclear whether the formation and movement of mRNP granules vary in different cell types (Rajgor and Shanahan, 2014).

To study the role of microtubules in mRNP granules, nocodazole has been used to cause microtubule disruption in cells. There is currently no study on the effect of post-translational modification of tubulin on the mRNP granules. Given the PTM of tubulin can affect microtubule stability, for example, de-tyrosination in tubulin is found in stable microtubules (Magiera and Janke, 2014). It can be an alternative way to study the role of microtubules in mRNP granules. A recent study in a gene called *Tacc3* showed the loss of TACC3 resulted in stable de-tyrosinated microtubules and impart cargo sorting (Furey et al., 2020). It may provide an alternative model to study whether microtubule dynamics impact the RNA granules.

1.3.3. P-bodies

Processing bodies (P-bodies) are one type of mRNP granules associated with mRNA degradation, translation repression, and mRNA storage. The components of P-bodies can be classified into a conserved core of proteins, miRNA repression factors, and translation repressors (Parker and Sheth, 2007). The conserved core includes protein such as the decapping enzyme DCP1a, decapping activator DDX6, and exonuclease Xrn1 (Parker and Sheth, 2007). The miRNA repression factors include miRNA silencing protein such as Argonautes and the translation repressors include proteins such as CPEB, staufen, and eIF4E (Parker and Sheth, 2007). Depletion of some of the protein components leads to an increase in P-bodies, such as LSM14b (Ayache et al., 2015), DCP2, and XRN1 (Eulalio et al., 2007). Whereas depletion of some of the protein components leads to a decrease in P-bodies, such as DDX6, LSM14a (Ayache et al., 2015), and CPEB1 (Serman et al., 2007). It is though unknown whether the change in number of P-bodies is a compensation for function or the loss in structural protein.

The exact function of P-bodies remains controversial, but it can be classified into mRNA degradation and mRNA storage. The association of P-bodies with mRNA degradation was based on the localization of decapping factors and decay intermediate in P-bodies (Sheth and Parker, 2003). However, it was also pointed out mRNA decay and RNA-mediated gene silencing remained functional in the absence of microscopic P-bodies (Eulalio et al., 2007). Recent single molecule imaging revealed that mRNA decay takes place throughout the cytoplasm and only intact transcripts were observed in P-bodies (Horvathova et al., 2017). Interestingly, it was also suggested that some mRNA with high AU content tends to be enriched in P-bodies and controlled at the level of translation (Courel et al., 2019). Although further studies will be required to confirm sequence specificity in the mode of regulation, it raised the question against the initial hypothesis of mRNA decay may be more efficient or inhibited within P-bodies and how decapping activities are inhibited in P-bodies. Given the evidence in the lack of mRNA decay activities in P-bodies (Horvathova et al., 2017, Hubstenberger et al., 2017), the role of storage granules may be more prominent in P-bodies. Most translation initiation factors are absent in P-bodes, except eIF4E, which is important in controlling the cap-dependent translation initiation (Andrei et al., 2005, Jackson et al., 2010). The eIF4E-binding protein, 4E-T, was also present in P-bodies and inactivate eIF4E (Andrei et al., 2005), suggesting the translation repression in P-bodies. Moreover, microRNA and Argonaute proteins are also found in P-bodies (Sen and Blau, 2005) and coimmunoprecipitated with P-bodies components such as DCP1A (Liu et al., 2005b). However, similar to the study of P-bodies in mRNA decay, some studies suggest P-bodies are not needed for the mediation of translation repression (Chu and Rana, 2006, Eulalio et al., 2007). It is not well-understood whether the presence of P-bodies in cells is a cause or consequence and whether there is any functional implication for the difference in P-bodies.

1.3.4. Stress granules

Stress granule is another type of mRNP granules that are induced with stress such as heat shock, nutrient starvation, and hypoxia (Reineke and Neilson, 2019). Unlike P-bodies, stress granules contain a number of translation initiation factors, such as eIF2, eIF3, eIF4A, and many of the stress granule proteins are not RNA binding proteins (Tian et al., 2020). Some markers for stress granules include TIA-1, G3BP1, and eIF3, which are absent in P-bodies (Hubstenberger et al., 2017). Similar to P-bodies, stress granules contain non-translating mRNA, with the presence of 40S ribosomal proteins and the absence of 60S ribosomal proteins (Kimball et al., 2003). Because of the ability to form the stress granules and the co-localization with repressed mRNA, the function of the stress granules has been proposed to be translation repression. However, recent live cell imaging analysis also reveals some mRNA inside stress granules can recruit 60S ribosome subunits and undergo translation (Mateju et al., 2020). The exact function of stress granules is also unclear. Given the depletion of stress granule markers, such as G3BP1 and G3BP2, can still inhibit translation without the formation of stress granule (Kedersha et al., 2016), it once again raises the question of whether these membrane-less structures are required for the function. One proposed function of the mRNP granules is the sequestration of proteins to alter cytosolic concentration (Hofmann et al., 2021). Indeed, the re-localization of proteins can affect the involvement in the signalling pathway. With the current development in APEX-based proximity labelling technique coupled with mass spectrometry, the interactome during stress and unstress conditions may be addressed to further elucidate the function of these mRNP granules.

1.4. Role of DEAD-Box Helicase 6 in translational control

To study the role of mRNP granules, DDX6 is one of the candidates due to its presence inside the granules. In addition, it has been suggested to mediate translational repression without the mRNP granules (Chu and Rana, 2006), making it an increasing candidate to study translational control.

1.4.1. DEAD box RNA helicase family

DEAD box proteins are named after the letter sequence of the amino acid in the protein's motif (Linder et al., 1989). Motif I and motif II contain the Walker A and Walker B motif respectively, which are found in ATP-binding protein (Walker et al., 1982). Further sequence analysis classified DEAD box proteins into the helicase superfamily 2 (Gorbalenya and Koonin, 1993). Numerous structural studies have shown a highly conserved helicase core in the DEAD box family, with a cleft formed between the two helicase domains harbouring the ATP-binding site and the associated RNA bound to the opposite (Linder and Jankowsky, 2011). The RNA binding ability is modulated by the ATP and ADP concentration, with high affinity in the presence of ATP and low in the presence of ADP (Yang and Jankowsky, 2005). Contrary to other DNA and RNA helicases, DEAD box proteins are not processive helicases. They unwind duplex using a distinct mode called local strand separation, which allows local structural change in RNA and RNA-protein complexes (Yang et al., 2007). Depending on the ATP binding and hydrolysis cycle, RNA binding or duplex unwinding can be accomplished (Nielsen et al., 2009).

Different functions of the DEAD box proteins have been described, ranging from transcription to translation or RNA export to RNA decay (Linder and Jankowsky, 2011). The DEAD box family is required in various steps in RNA metabolism. In addition, this gene family has also been found to be dysregulated in cancer and involved in differentiation

(Abdelhaleem et al., 2003). In this study, I will focus on one of its members, DDX6, which is involved in RNA storage and RNA decay (Minshall et al., 2009).

DEAD-Box Helicase 6 is one of the members of the DEAD box proteins. Different homologs of DDX6 have been studied: ME31B in *Drosophila melanogaster* (de Valoir et al., 1991), Xp54 in *Xenopus* oocytes (Ladomery et al., 1997), DHH1 in *Saccharomyces cerevisiae* (Strahl-Bolsinger and Tanner, 1993). The common feature between these homologs is their presence in mRNP particles (Weston and Sommerville, 2006). A recent clinical study on missense variant of DDX6 showed neurodevelopmental syndrome with defects in P-body assembly (Balak et al., 2019), suggesting the importance of DDX6 in RNA regulation.

1.4.2. DDX6's role in translation repression

Different studies have been conducted to study the role of DDX6 in translation repression. Since DDX6 is one of the key components in P-bodies, some studies focused on the role of DDX6 in translation repression. In human cells, it is suggested that DDX6 represses global translation and mRNA-specific translation and such repression is not mediated by P-bodies (Chu and Rana, 2006). Though the proposed model is still debatable. In another study, knockdown of GW182, a component in P-bodies, impaired miRNA-mediated translation repression (Liu et al., 2005a). However, GW182 is also found in miRISC, making it difficult to determine if the impact in silencing was due to the disruption of P-bodies or miRISC. In pluripotent stem cells, a similar observation is seen. Knockdown of DDX6 or the structural component in P-bodies, such as LSM14A both resisted pluripotency exits and increased expression of transcripts repressed in the granules (Di Stefano et al., 2019). Once again suggesting the mediation of the translation repression through P-bodies. The difference in phenotype observed can be due to cell types, involvement in microRNA, or the approach

to identifying P-bodies. Across different studies, different markers have been used to look at the P-bodies after knockdown studies. Although some studies showed the effect of knocking down different components in P-bodies (Ayache et al., 2015), there is no consensus on what marker can definitively mark the presence of the granules, only the localization of the selected P-bodies component. Hence, it remains difficult to conclude the role of DDX6 in the context of P-bodies. However, it is interesting to note that DDX6 seems to regulate protein expression by binding to the mRNA. In eCLIP analysis, DDX6 preferentially binds to the coding sequence of mRNA (Di Stefano et al., 2019). In another study, DDX6 was shown to interact with *Vegf* mRNA 5' UTR and repress *Vegf* translation in normoxic conditions (de Vries et al., 2013). Depletion of DDX6 by RNAi or inducing hypoxia increases the expression of *Vegf* (de Vries et al., 2013). It may be suggesting the repression by DDX6 may be partially sequence specific.

Other studies focused on the role of DDX6 in immunology. DDX6 has been reported to be involved in multiple viruses, for example, depletion of DDX6 has been shown to decrease the abundance of hepatitis C virus proteins (Pager et al., 2013). Depletion of P-bodies proteins or stress granules components also decreased the overall abundance of hepatitis C virus RNA (Pager et al., 2013). Further study in genome-wide interferon-stimulated gene suppressor screen identifies DDX6 as a suppressor (Lumb et al., 2017). Deletion of DDX6 induces an antiviral state, which may suggest a role in sensing viral infection (Lumb et al., 2017). Interestingly, VCAM1, a marker used in satellite cells isolation, was upregulated in DDX6 knockout cells (Lumb et al., 2017). Knockout of VCAM1 in satellite cells has been suggested to impair regeneration and increase apoptosis (Choo et al., 2017). *In vivo*, it is hypothesized the satellite cells interact with immune cells through VCAM1 binding to α4β1 integrin to promote cell expansion during injury (Choo et

al., 2017). Changes in VCAM1 in DDX6 knockout satellite cells may give us more insights into the role of DDX6 in satellite cells.

1.4.3. DDX6's role in primary myoblast

The role of DDX6 in primary myoblast was studied through ATAC-seq and eCLIP experiments (Di Stefano et al., 2019). ATAC-seq analysis revealed the knockdown of DDX6 had an overall increase in chromatin accessibility at enhancer regions, which includes regions associated with myogenic differentiation (Di Stefano et al., 2019). One of the targets, *Kdm4b*, was upregulated during DDX6 knockdown, and depletion of KDM4B inhibited differentiation (Di Stefano et al., 2019). A similar result with an increase in expression of differentiation genes such as myogenin was also reported (Wang et al., 2015). In addition, DDX6 was shown to facilitate the translation of genes related to proliferation such as CDK1 and EZH2 (Wang et al., 2015). In satellite cells, DDX6 has only been used to identify the mRNP granules in satellite cells (Crist et al., 2012; Goel et al., 2017). During satellite cell activation, the DDX6 (+) puncta decreased and showed a more cytoplasmic staining (Crist et al., 2012). However, there is currently no study focusing on the function of DDX6 in satellite cells. It is unknown whether DDX6 acts only by repressing mRNA translation, such as *Myf5* (Crist et al., 2012), or it can have other functions. Moreover, it is also unknown whether other mRNAs are repressed similarly to Myf5 in satellite cells and how the function of DDX6 changes during the myogenic program, given the protein is still present after activation. Study of the DDX6 may help us further understand how quiescence and regeneration are regulated.

1.5. Hypothesis and Objectives

Several experimental approaches are used to understand how muscle stem cells exit quiescence and re-enter quiescence at the epigenetic, transcriptional, and translational levels (Massenet et al., 2021; Relaix et al., 2021; Zismanov et al., 2016). Given the translational level can provide a rapid accumulation of proteins during early activation through the dissolution of mRNP granules (Crist et al., 2012), I aim to investigate the regulation at the translational level.

From mass spectrometry and RNA-seq results in satellite cells cultured in sal003 versus DMSO, a set of genes was identified to have increased protein level without increase in mRNA level in the sal003 condition (Fujita et al., 2021), suggesting these genes may be preferentially translated when the eIF2α is phosphorylated. One of the genes, *Tacc3*, was shown to have uORFs that enable *Tacc3* mRNA translation when eIF2α levels are maintained by the addition of sal003 in *ex vivo* culture conditions (Fujita et al., 2021). Whether or not *Tacc3* mRNA is also selectively translated in quiescent MuSCs, which also have a high eIF2α level (Zismanov et al., 2016), remains unclear. Therefore, I hypothesized that *Tacc3* is selectively translated in quiescent satellite cells and has a function in the quiescence of satellite cells. To investigate the role of TACC3 in quiescent satellite cells, immunofluorescence staining will be used to look at the protein level in quiescent and activated satellite cells. Inducible knockout mice will be used to knock out TACC3 in satellite cells and the number of quiescent satellite cells will be quantified to look at the effect on quiescence maintenance.

One of the studies on TACC3 showed the loss of TACC3 increased the portion of stable de-tyrosinated microtubules and impaired cargo transport in a neuroblastoma cell line (Furey et al., 2020). Kinesin-1 activity was shown to be higher in the loss of TACC3 (Furey

et al., 2020), which is likely to be caused by preferential motility of kinesin on stable de-tyrosinated microtubules (Cai et al., 2009). Given the localization of mRNP granules on microtubules (Aizer et al., 2008), the transport of mRNP granules may also be impaired if the microtubule network is changed. Therefore, I hypothesized that TACC3 have a role in maintaining a dynamic microtubule structure and cargo transport in quiescent satellite cells, and knockout of TACC3 will cause the formation of stable de-tyrosinated microtubules structure and impair mRNP granules disassembly and quiescence exit. To investigate whether loss of TACC3 will cause the formation of stable de-tyrosinated microtubules, inducible knockout mice will be used to knockout TACC3 in satellite cells and the de-tyrosinated microtubules network will be visualized by immunofluorescent staining using an antibody against de-tyrosinated α-tubulin.

The second part of the thesis focused on one of the major components of mRNP granules, DDX6, to further understand the translational control in MuSCs. DDX6 was used to identify mRNP granules in satellite cells and DDX6 granules were shown to disassemble during satellite cell activation (Crist et al., 2012; Goel et al., 2017). However, there is currently no study on the function of DDX6 in satellite cells. Given that DDX6 has been shown to mediate both global translation repression and mRNA-specific translation repression in other cell types (Chu and Rana, 2006) and global translation repression was shown to be important in quiescent satellite cells (Zismanov et al., 2016), I hypothesized that DDX6 play a role in quiescence maintenance through translation repression. It is currently not known how the mRNP granules changes as the myogenic progenitors establish quiescence. Given the presence of DDX6 mRNP granules in quiescent satellite cells, I hypothesized that during postnatal growth, acquisition of DDX6 mRNP granules in myogenic progenitors is needed to establish quiescence. To validate whether the myogenic progenitors

acquire mRNP granules as they establish quiescence, immunofluorescence staining will be used to look at the number of DDX6 granules at different timepoints during postnatal growth.

Though the DDX6 granules were shown to disassemble during the satellite cell activation (Crist et al., 2012), it is not known whether the granules will reassemble as the myogenic program proceed and if so, will there be a change in composition. A study of DDX6 in human myoblast cell line showed the role of DDX6 in suppressing differentiation of myoblast through targeting a transcript encoding a chromatin-remodeling enzyme, KDM4B, which targets the differentiation gene Myogenin (Di Stefano et al., 2019). However, it is not known whether the increase in differentiation is mediated through mRNP granules. Given the role of DDX6 in translation repression during differentiation, I hypothesized the mRNP granules will reassemble during the myogenic program to sequester mRNA required in differentiation. To investigate how the granules change during the myogenic program, immunofluorescence staining will be used to visualize the number of DDX6 granules in cultured satellite cells. In addition, DCP1a will be used to visualize the changes in P-bodies during the myogenic program. Lastly, given the study of DDX6 was in a cell line and the model of study in this thesis is primary cells, knockdown of DDX6 in freshly isolated satellite cells will be used to validate the role of DDX6 in differentiation and to investigate how different myogenic populations will be impacted.

Chapter 2: Materials and Methods

2.1 Mice

Tacc3$^{fl/fl}$ mice were a gift from R. Yao (Yao et al., 2016). *Pax7*$^{CreERT2/+}$ mice (Murphy et al., 2011) and *Rosa26*^{tdTomato} (Madisen et al., 2009) mice were purchased from Jackson Laboratories. All the mice were maintained on a C57/Bl6 background. Swiss mice were purchased from Charles River Laboratories. Animal care was performed in accordance with the guidelines of the Canadian Council on Animal Care (CCAC).

2.2 Tamoxifen injection

Tamoxifen was prepared in corn oil and 30% ethanol. It was administered through intraperitoneal injections (2mg/day) for 5 consecutive days and maintained on a tmx diet.

2.3 TA muscle freezing and Cryo-sectioning

TA muscle was fixed in 0.5% paraformaldehyde at 4℃ for 2 hours and then transferred to 20% sucrose at 4℃ overnight. On the next day, it was mounted in Frozen Section Compound and frozen in isopentane, which was pre-chilled in liquid nitrogen. Frozen TA muscle was stored at -80℃. TA muscle was sectioned with a thickness of 10µm using the Cryostat.

2.4 Isolation of satellite cell using Fluorescence-Activated Cell Sorting

Satellite cells were isolated from the diaphragm and abdominal muscle of adult *Pax3*$^{GFP/+}$ mice as previously described (Zismanov et al., 2016) using the BD FACSAria Fusion cell sorter. The satellite cells were stained with propidium iodide to exclude dead cells and sorted with the FITC channel to gate the GFP+ cells.

2.5 Cell culture

Isolated satellite cells were plated on 0.2% gelatin-coated culture plate and cultured in 39% DMEM, 39% F12, 20% FBS, 2% UltroserG for 4 days unless indicated.

2.6 Single fiber preparation and culture

EDL muscle was digested in 0.5% collagenase D with DMEM at 37℃ for 50 minutes for all postnatal timepoints and dissociated in DMEM with 10% FBS. The single fibres are cultured in DMEM, 39% F12, 20% FBS, 2% UltroserG for 6, 24, 48 or 72 hours.

2.7 Immunofluorescence

Isolated satellite cells were fixed in 10% formalin, followed by permeabilization in 50mM ammonium chloride with 0.2% Triton X and blocked in 0.2% gelatin.

Isolated EDL myofibers were fixed in 10% formalin, followed by permeabilization in methanol, incubation in 50mM ammonium chloride, and blocked in 5% horse serum.

TA cryosections were permeabilized in 0.1% Triton X and 0.1M glycine and blocked in M.O.M reagent.

2.8 Western Blotting

Cells were lysed in RIPA buffer supplemented with cOmplete protease inhibitor and phosphatase inhibitor. Supernatant was collected by centrifugation for 21 mins at 4℃ and boiled in NuPAGE LDS Sample Buffer (Invitrogen) and NuPAGE Sample Reducing Agent (Invitrogen) for 10 mins at 70℃. Cell lysates were resolved using SDS-PAGE and transferred onto a PVDF membrane. Membrane was blocked in 5% BSA in 0.1% TBST. Primary antibodies were incubated overnight at 4℃ and secondary antibodies were incubated for 1 hour at room temperature. TBST washes were performed after antibody incubation. Membrane was visualized using ECL Prime Western Blotting Detection reagents (GE Healthcare) and ChemiDoc (Bio-Rad Laboratories).

2.9 Molecular Cloning

shRNA targeting DDX6 mRNA were designed, and a scrambled sequence was used as control. Two primers were annealed and cloned into pLKO-RFP-shCntrl plasmid (Addgene

plasmid #69040) digested with KpnI and EcoRI using T4 ligase (Invitrogen). The following shRNA target sequences were used for DDX6 silencing:
shDDX6: GACAAACTACAGAAGGCTCTT and GCAGATAATGGAGGATATTAT
scrambled: GGCAAGTTATACCCGTAAACA

pLKO-RFP-shCntrl was a gift from William Kaelin (Addgene plasmid # 69040 ; http://n2t.net/addgene:69040 ; RRID:Addgene_69040)

2.10 Lentiviral Transduction

HEK293T cells were transfected with the shDDX6 or scrambled shRNA plasmids using jetPRIME® transfection reagent (Illkirch-Graffenstaden). 6 hours after transfection, the medium was changed to satellite cell medium (DMEM, 39% F12, 20% FBS, 2% UltroserG) and cultured for 24 hours. Supernatant was collected and filtrated through a 0.45µm filter. Satellite cells were transduced with 1mL of lentiviral solution supplemented with polybrene (5 µg/ml). 18 hours after transduction, the lentivirus containing medium was removed and replaced with fresh satellite cell medium. Transduced cells were cultured for an additional 3 days.

2.11 Antibodies

Primary antibodies were against PAX7 [Developmental Studies Hybridoma Bank (DSHB) 1:100], MYOD (Santa Cruz Biotechnology, sc-377460, 1:200), MYOG (Abcam, 124800, IF: 1:300, WB: 1:2000), TACC3 (Abcam, 134154, 1:200), laminin (Sigma-Aldrich, L9393, 1:500), Ki67 (Abcam, ab16667, 1:250), Detyrosinated α-tubulin (abcam, ab48389, 1:250), β-tubulin (EMD Millipore, 05-661, 1:200), DDX6 (Bethyl, A300-461A, IF:1:500, WB:1:2000), DCP1a (Santa Cruz Biotechnology, sc-100706, IF: 1:200, WB: 1:500), β-actin (Sigma-Aldrich, A5441, 1:2000).

For immunofluorescence, secondary antibodies were against Alexa Fluor-488, Alexa Fluor-594 and Alexa Fluor-647 conjugated secondary anti-mouse IgG1, anti-mouse IgG, IgG2a and IgG2b or anti-rabbit (Life Technologies, A21121, A-21125, A-21135, A21145 and A31573, 1:500). For western blotting, horseradish peroxidase (HRP)-conjugated anti-mouse or anti-rabbit secondary antibodies (Jackson ImmunoResearch, 115-035-003 and 111-035-003, 1:10000) were used.

2.12 Statistical Analysis

Graphs are represented as mean ± s.e.m. Unless indicated, three independent replicates of each experiment were performed. Unless indicated, significance was calculated by unpaired Student's t-tests with two-tailed P values: *P<0.05, **P<0.01, ***P<0.001. Unless indicated, there was no significant difference between the data. Pearson correlation coefficient was performed with two-tailed P values: *P<0.033, **P<0.002, ***P<0.001.

2.13 Quantification Parameters

For the EDL myofiber data, cells were considered positive for the markers (PAX7, MYOD, or KI67) if the average signal intensity is more than two-fold of the measured background intensity using the myofiber as a reference. All the images for the granules were imaged with ZEISS LSM 800 Microscope with a 63X objective and 4X averaging. For the quantification of the number of DDX6 granules, all the granules quantified have a minimum area of $0.02\mu m^2$ on the maximum orthogonal projection image, which is approximately 160nm in diameter, however, the granules were not all circular, so it was difficult to determine their diameter. The average intensities of granules were at least two-fold the measured background intensity.

Chapter 3: Results

3.1 TACC3 and the microtubule structure in quiescent satellite cells

Through mass spectrometry and RNA-seq data in satellite cells cultured in sal003 versus DMSO, *Tacc3* was identified to have increased protein level without change in mRNA level in the sal003 condition (Fujita et al., 2021). Moreover, *Tacc3* was shown to have uORFs in the 5' region of the transcript that enable *Tacc3* mRNA translation when P-eIF2α is maintained by sal003 (Fujita et al., 2021). Given quiescent satellite cells were reported to have high P-eIF2α level (Zismanov et al., 2016), TACC3 may play a role in quiescent satellite cells. Therefore, in the first part of the thesis, I aimed to study the role of TACC3 in quiescent satellite cells.

First, I assessed whether TACC3 plays a role in the maintenance of quiescence. By utilizing inducible knockout mice, TACC3 was knocked out in quiescent satellite cells to study the effect on quiescence maintenance. TA muscle was harvested from tamoxifen-treated $Pax7^{CreERT2/+}$ and $Pax7^{CreERT2/+};Tacc3^{fl/fl}$ mice (Figure 2A). Through immunofluorescence staining, no change in the number of satellite cells within the laminin and outside the laminin was observed 21 days after tamoxifen injection, suggesting TACC3 does not play a role in maintaining quiescence in satellite cells (Figure 2B-C). Next, I asked whether TACC3 is expressed in quiescent satellite cells. Weak cytoplasmic staining of TACC3 was observed in PAX7 expressing cells on freshly isolated myofiber (Figure 2D). To further look at the expression of TACC3, immunofluorescence analysis in cultured myofiber showed clear staining in PAX7 expressing cells after 24 and 48 hours of culture (Figure 2E). Here, only the PAX7 expressing cells with clear TACC3 staining were considered TACC3 positive. The percentage of PAX7 cells expressing TACC3 increased significantly from an

average of 56% after 24 hours of culture to 96% after 48 hours of culture (Figure 2F), suggesting TACC3 plays a role in the myogenic program.

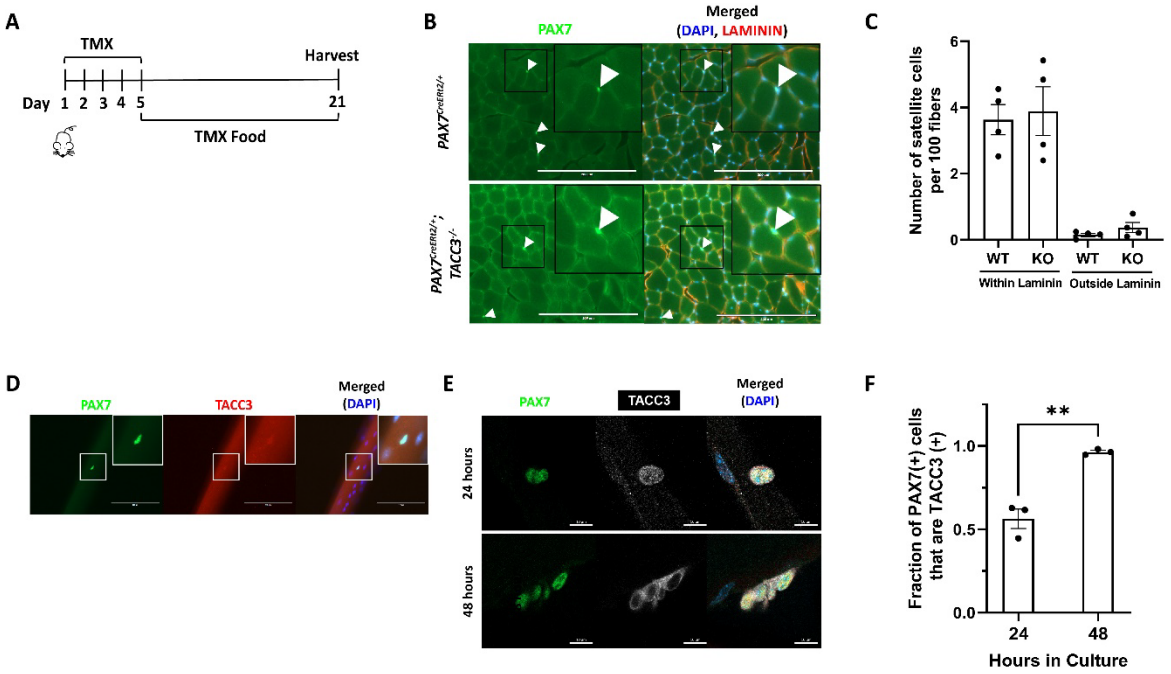

Figure 2. TACC3 is expressed during satellite cells activation.

(A) Schematic illustration of the experiment.

(B) Representative immunofluorescence analysis of cryosection of tibialis anterior (TA) muscles of *Pax7*$^{CreERT2/+}$ and *Pax7*$^{CreERT2/+}$*; Tacc3*$^{fl/fl}$ mice (isolated from n=4 mice), with antibodies against PAX7 (green) and laminin (red). White arrow indicates PAX7 (+) cells within basal laminin.

(C) Quantification of the number of satellite cells within and outside the basal laminin in (B).

(D) Representative immunofluorescence analysis of a freshly isolated myofiber, with antibodies against PAX7 (green) and TACC3 (red).

(E) Representative immunofluorescence analysis of the isolated myofiber cultured for 24 hours (upper panel) and 48 hours (lower panel) (isolated from n=3 mice), with antibodies against PAX7 (green) and TACC3 (white).

(F) Quantification of fraction of PAX7(+) cells that are TACC3 (+) in E.

Data are mean ±sem. *P<0.05, **P<0.01, ***P<0.001 (unpaired two-tailed Student's t-test), no significance unless specified. Scale bars: 200 µm in B; 100 µm in D; 10 µm in E.

Loss of TACC3 was shown to increase the portion of stable de-tyrosinated microtubules and hence, impaired the cargo transport through altered kinesin mobility (Furey et al., 2020). Though TACC3 has low protein level in quiescent satellite cells, it may still affect the microtubule network and cause the formation of stable de-tyrosinated microtubule network and potentially impair the transport of mRNP granules and quiescence exit. To validate the hypothesis, first, I validated the de-tyrosinated α-tubulin antibody by co-staining β-tubulin with de-tyrosinated α-tubulin in freshly isolated myofiber from *PAX7*$^{CreERT2/+}$;*Rosa26*$^{tdTomato/+}$ mice. De-tyrosinated α-tubulin showed some overlapping with β-tubulin and some continuous lines were observed in the myofiber, indicating the de-tyrosinated α-tubulin staining was successful (Figure 3A). However, stable de-tyrosinated microtubules were not observed in both wild-type and TACC3 knockout satellite cells, suggesting knockout of TACC3 did not increase the portion of stable de-tyrosinated microtubules (Figure 3B) in satellite cells.

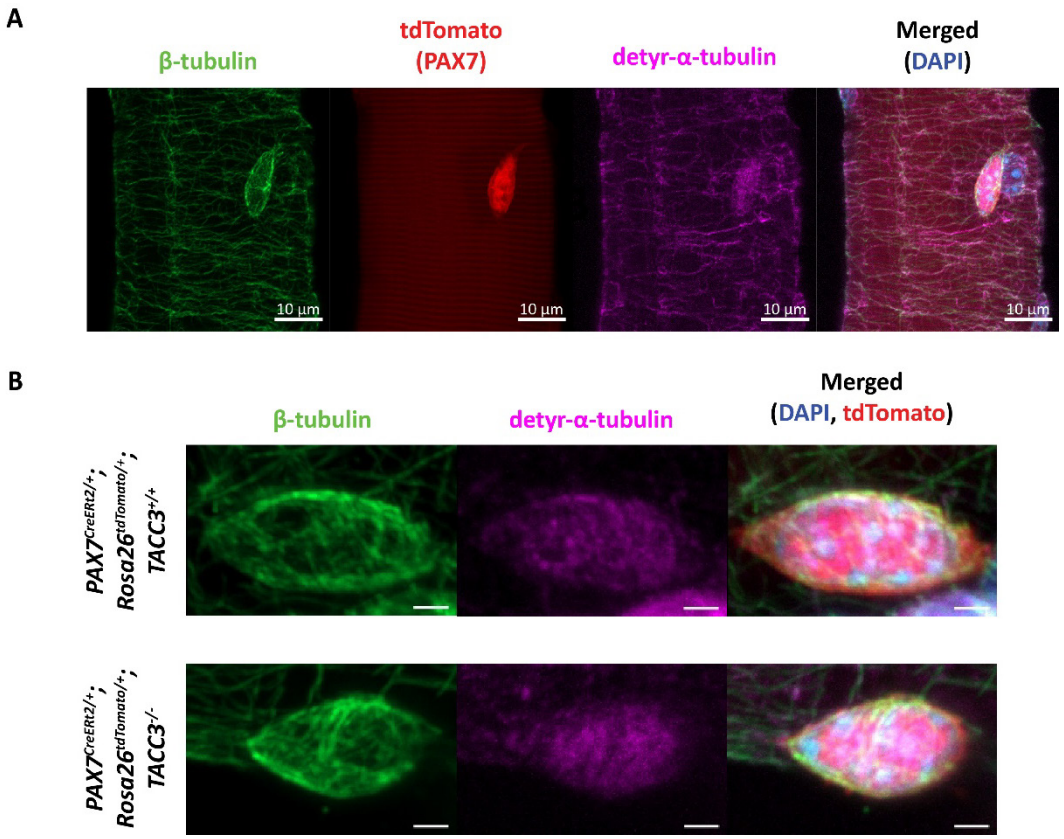

Figure 3. De-tyrosinated stable microtubule network is absent in both wild-type satellite cell and TACC3-knockout satellite cell.

(A) Representative immunofluorescence image of de-tyorsinated α-tubulin staining of freshly isolated EDL myofiber from the *PAX7*$^{CreERT2/+;}$*Rosa26*$^{tdTomato/+}$ mice, with antibodies against β-tubulin (green) and de-tyrosinated α-tubulin (purple).

(B) Representative immunofluorescence image of the freshly isolated myofiber from the *PAX7*$^{CreERT2/+;}$*Rosa26*$^{tdTomato/+}$;*TACC3*$^{+/+}$ mice (upper panel) and *PAX7*$^{CreERT2/+;}$*Rosa26*$^{tdTomato/+}$;*TACC3*$^{fl/fl}$ mice (lower panel), with antibodies against β-tubulin (green) and de-tyrosinated α-tubulin (purple).

Scale bars: 10μm in A; 2μm in B.

Knockout of TACC3 in quiescent satellite cells did not lead to observable phenotype and my data suggested TACC3 does not have a role in maintaining quiescence and dynamic microtubule network in quiescent satellite cells. However, TACC3 was shown to be important in muscle regeneration and self-renewal (Fujita et al., 2021). Given my research topic focused on the translational control of MuSCs, particularly the mRNP granules, the second part of my thesis focused on the role of DDX6 in MuSCs.

3.2 DDX6 granules during postnatal growth

In the second part of the thesis, DDX6, which is one of the major components of mRNP granules, is studied to investigate the translational control in MuSCs. Different studies have shown the presence of mRNP granules in quiescent satellite cells, through immunofluorescence staining of DDX6 (Crist et al., 2012; de Morrée et al., 2017; Fujita et al., 2017). The presence of granules during the translation repression (Zismanov et al., 2016) may suggest a functional role in quiescent satellite cells. Indeed, the sequestration of Myf5 transcript has been shown to be an example of DDX6 function in satellite cells through mRNP granules (Crist et al., 2012). To further investigate the potential role of DDX6 through mRNP granules, I first looked at how the number of granules changed during the establishment of quiescence in postnatal growth. Since DDX6 mRNP granules are present in

quiescent satellite cells, I hypothesized that during postnatal growth, acquisition of DDX6 mRNP granules in myogenic progenitors is needed to establish quiescence.

From literature, it was observed that PAX7 (+) MYOD (-) population increased significantly from postnatal day 21 and day 28 and all the myogenic progenitors became located under the basal laminin by postnatal day 28 (Gattazzo et al., 2020), signifying an important transition. Hence, I chose postnatal days 21, 28, and 56 as the timepoints to investigate, with day 56 representing fully quiescent satellite cells. Using DDX6 as a marker for mRNP granules, no significant difference were observed between the three time points (Figure 4A-B). Though there was no significance difference between the time points, the average number of DDX6 (+) granules in P21 was close to double of the average number in P28. Given during postnatal day 21 and 28, the PAX7 (+) cells are composed of different myogenic populations, I further asked if there is a difference in granules between PAX7 (+) MYOD (+) cells and PAX7 (+) MYOD (-) cells. Indeed, a significant drop in the number of granules was observed between the PAX7 (+) MYOD (+) cells in P21 and P28 whereas there was no significant difference between the PAX7 (+) MYOD (-) cells in P21 and P28 (Figure 4C-D). I further verified if there was a significant increase in the PAX7 (+) MYOD (-) cells as reported (Gattazzo et al., 2020). However, no significant difference in the fraction of PAX7 (+) MYOD (-) cells between P21 to P28 (Figure 4E). In addition, I checked if the decrease in number of granules resulted from a reduction in cell proliferation. However, there was also no significant difference in the fraction of PAX7 (+) KI67 (-) cells between P21 and P28 (Figure 4F).

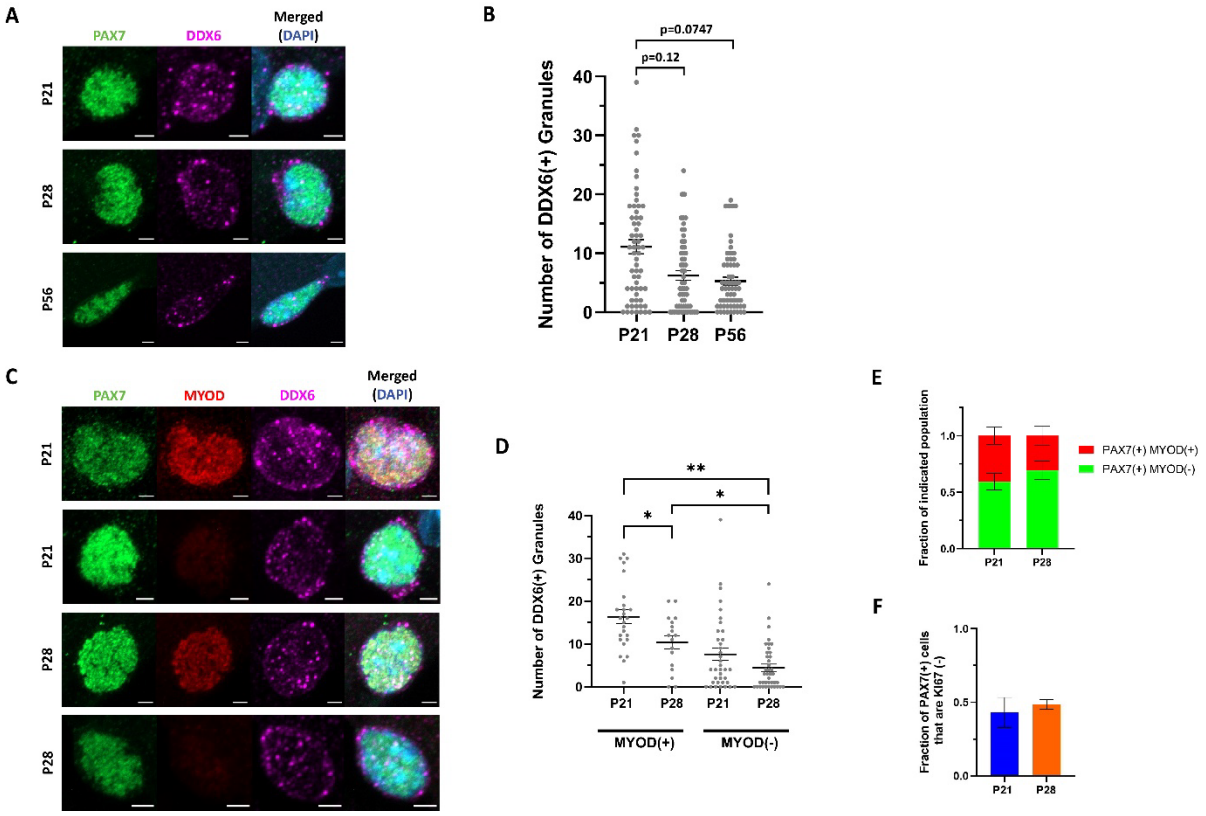

Figure 4. Change in number of granules in myogenic progenitors during postnatal growth.

(A) Representative immunofluorescence analysis of freshly isolated EDL myofiber from the postnatal day 21 (upper panel), postnatal day 28 (middle panel) and postnatal day 56 (bottom panel), with antibodies against PAX7 (green) and DDX6 (purple).

(B) Quantification of the number of DDX6 granules in (A).

(C) Representative immunofluorescence analysis of freshly isolated EDL myofiber from the postnatal day 21 (1st and 2nd panels) and postnatal day 28 (3rd and 4th panels), with antibodies against PAX7 (green), MYOD (red) and DDX6 (purple).

(D) Quantification of number of DDX6 granules in (C).

(E) Quantification of fraction of MYOD (+) and MYOD (-) population in (C).

(F) Quantification of fraction of PAX7(+) KI67(-) population in postnatal day 21 and day28 in freshly isolated EDL myofiber.

Data are mean ±sem. *P<0.05, **P<0.01, ***P<0.001 (unpaired two-tailed Student's t-test), no significance unless specified. Scale bars: 2µm in A and C.

3.3 DDX6 granules during the myogenic program in adult satellite cells

DDX6 granules were shown to disassemble during the satellite cell activation (Crist et al., 2012). However, it is not known how the granules change as the myogenic program proceeds. In human myoblast, DDX6 has been shown to be involved in differentiation (Di Stefano et al., 2019). Moreover, it was unexpected that a higher number of granules was observed in PAX7(+) MYOD(+) cells since disassembly of granules was reported during satellite cell activation (Crist et al., 2012). Therefore, the change in mRNP granule number and type during the myogenic program is further investigated here through DDX6.

I first focused on the number of DDX6 granules in adult quiescent satellite cells since a discrepancy in the number of DDX6 granules was observed, with an average of around 7 granules per cell reported in literature (Crist et al., 2012). Here, I observed several satellite cells with relatively weaker PAX7 staining and the number of granules was also fewer (Figure 5A and B). To ask if there is any correlation, the average fluorescence intensity of PAX7 and the number of granules were quantified and subjected to Pearson's correlation analysis. A significant positive correlation was found between the average fluorescence intensity of PAX7 and the number of granules, with a correlation value of 0.6111 (Figure 5B).

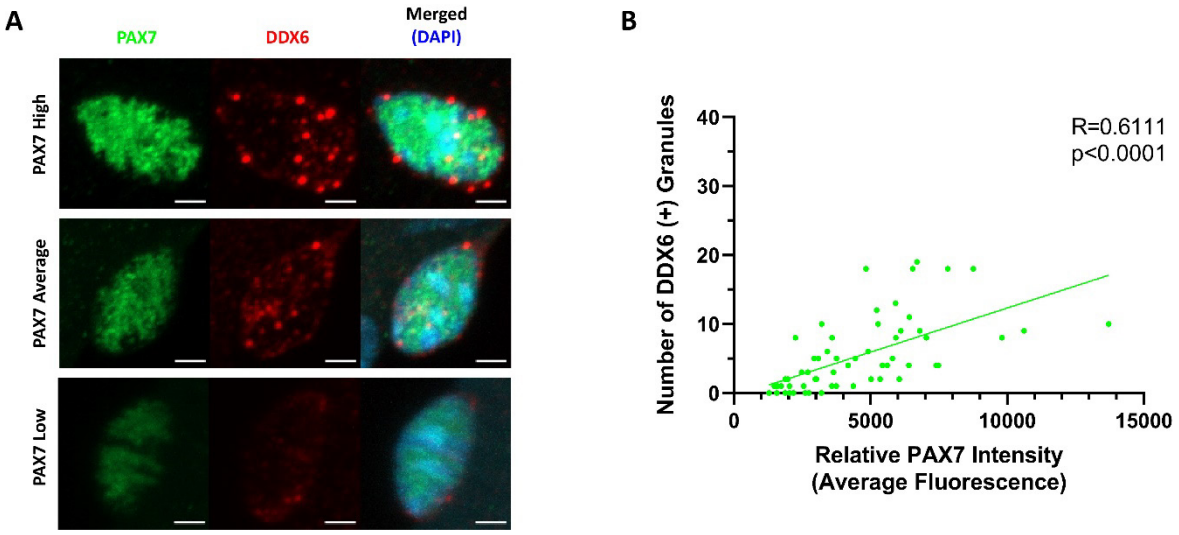

Figure 5. Number of DDX6 granules is positively correlated with PAX7 level in quiescent satellite cells.

(A) Representative immunofluorescence analysis of freshly isolated EDL myofiber from the postnatal day 56, with antibodies against PAX7 (green) and DDX6 (red). Different panels show different intensities of PAX7 in satellite cells, PAX7 High (upper panel), PAX7 Average (middle panel) and PAX7 Low (bottom panel).

(B) Pearson's correlation coefficient between the number of DDX6 granules and relative average fluorescence intensity of PAX7.

*P<0.033, **P<0.002, ***P<0.001 (unpaired two-tailed Student's t-test). Scale bars: 2μm in A.

The change in number of DDX6 granules during activation was then investigated. I compared the number of DDX6 granules in satellite cells from freshly isolated myofiber, myofibers cultured for 6 hours and 24 hours. No significant change in the number of granules was observed from 0 hours to 6 hours in culture (Figure 6A-B). However, from 6 hours to 24 hours of culture, a significant increase in the number of granules was observed. In addition, stronger cytoplasmic staining was observed in 24 hours compared to 0 hour and 6 hours of culture. Since a correlation was found between PAX7 and the number of granules in quiescent satellite cells, I asked if a similar correlation can be observed in activated satellite. I quantified the average fluorescence intensity of PAX7 in PAX7 expressing cells at 0, 6, and 24 hours of culture. The average fluorescence intensity of PAX7 significantly drops from 0

hours to 24 hours. No significant decrease was observed from 0 hours to 6 hours (Figure 6C). Pearson's coefficient analysis was subsequently performed on PAX7 expressing cells from 0 hours and 24 hours of culture. The correlation observed in quiescent satellite cells was not present after 24 hours of culture, with a correlation value of 0.1358 without any significance (Figure 6D).

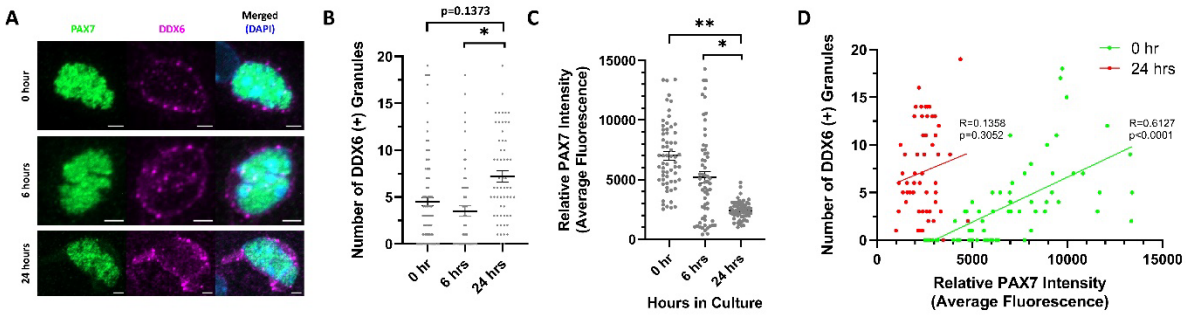

Figure 6. Number of DDX6 granules increases during activation in adult satellite cells.
(A) Representative immunofluorescence analysis of freshly isolated and cultured EDL myofiber from adult mice, with antibodies against PAX7 (green) and DDX6 (red). Different panels show different culture times, 0 hours (upper panel), 6 hours (middle panel) and 24 hours (bottom panel).
(B) Quantification of the number of DDX6 (+) granules in (A).
(C) Quantification of the relative average fluorescence intensity of PAX7 in (A).
(D) Pearson's correlation coefficient between the number of DDX6 granules and relative average fluorescence intensity of PAX7 in (A).
For B and C: Data are mean ±sem. *P<0.05, **P<0.01, ***P<0.001 (unpaired two-tailed Student's t-test). For D: *P<0.033, **P<0.002, ***P<0.001 (two-tailed P value), no significance unless specified. Scale bars: 2μm in A.

3.4 P-bodies during the myogenic program

Since a significant increase in the number of granules was observed from 6 hour to 24 hours of culture, I asked whether there is a change in the type of granule. A change in granule formation was hypothesized to have a direct correlation with the concentration of the components of granules (Luo et al., 2018). In one study, it was shown that non-quiescent

cells possessed a higher number of granule structures, such as P-bodies (Lee et al., 2016). I, therefore, assessed if the higher number of granules was caused by an increase in the components of P-bodies and hence, an increase in P-bodies. To verify my hypothesis, I did bioinformatics analysis using RNA-seq data (Yue et al., 2020) for *Dcp1a*, which is a marker for P-bodies. *Dcp1a* transcript was indeed enriched in activated satellite cells compared to fixed quiescent satellite cells (Figure 7A). In satellite cells from 0 hours and 24 hours cultured myofiber, staining with DDX6 and DCP1a showed a significant increase in the fraction of DDX6 granules that were also DCP1a (+), with an average of 0.32 in 0 hours and an average of 0.67 in 24 hours of culture (Figure 7B-C). In addition, a stronger DCP1a puncta staining was also observed after 24 hours of culture (Figure 7B).

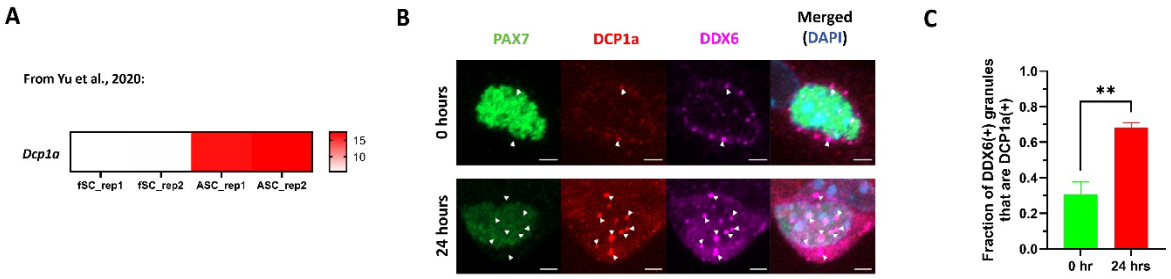

Figure 7. DDX6 granules shift to P-bodies during activation.

(A) Heatmap of *Dcp1a* transcript level from data from Yue et al., 2020, the two datasets on the left represent the fixed satellite cells (fSC) and the two datasets on the right represents activated satellite cells (ASC). The values are in FPKM.

(B) Representative immunofluorescence analysis of freshly isolated and cultured EDL myofiber from adult mice, with antibodies against PAX7 (green), DCP1a (red) and DDX6 (purple). The upper panel is 0 hour, and the lower panel is 24 hours.

(C) Quantification of fraction of DDX6(+) granules that are DCP1a (+) from (A).

Data are mean ±sem. *P<0.05, **P<0.01, ***P<0.001 (unpaired two-tailed Student's t-test). Scale bars: 2μm in A and B.

To see if a similar observation is present in postnatal myogenic progenitors, I also compared myogenic progenitors from P21 and P56 to look at the fraction of DDX6 (+)

granules that are also DCP1a (+). However, no significant difference was observed (Figure 8A-B).

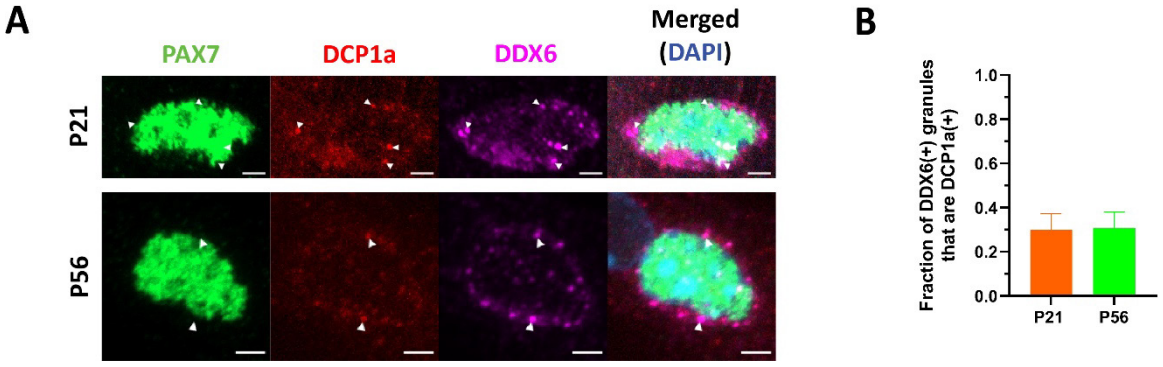

Figure 8. Fraction of P-bodies in myogenic progenitors during postnatal growth
(A) Representative immunofluorescence analysis of freshly isolated EDL myofiber from the postnatal day 21 (upper panel) and postnatal day 56 (lower panel), with antibodies against PAX7 (green), DCP1a (red) and DDX6 (purple). The white arrow represents the DDX6 (+) DCP1a (+) granule.
(B) Quantification of fraction of DDX6(+) granules that are DCP1a(+) from (A).
Data are mean ±sem. *P<0.05, **P<0.01, ***P<0.001 (unpaired two-tailed Student's t-test), no significance unless specified. Scale bars: 2μm in A and B.

3.5 Effect of DDX6 Knockdown

DDX6 was shown to play a role in differentiation in human myoblast cell line (Di Stefano et al., 2019). Given primary cells and cell line can have different behaviour, I investigated the effect of DDX6 knockdown in freshly isolated satellite cells. Using lentiviral particles, I transduced the satellite cells with shRNA targeting DDX6 and a scrambled shRNA sequence as control and cultured the cells for 4 days in total (Figure 9A). I verified the knockdown efficiency by using western blotting, the average protein level of DDX6 in shDDX6 significantly reduced to one-third of the scrambled control (Figure 9B-C). A significant increase in the level of MYOGENIN was observed in shDDX6 compared to the scrambled control (Figure 9B and 9D). Next, I asked whether the change in myogenin was accompanied by a change in the myogenic population. Immunofluorescence analysis was

consistent with the western blotting result, a significant increase in the PAX7(-) and MYOGENIN (+) population was observed in the shDDX6 condition compared to the scrambled control (Figure 9G-H). Lastly, I asked if the change in myogenic population resulted in a change in the size of the colony. I quantified the number of cells in each colony and a significant decrease in the number of cells in the shDDX6 condition was observed (Figure 8I).

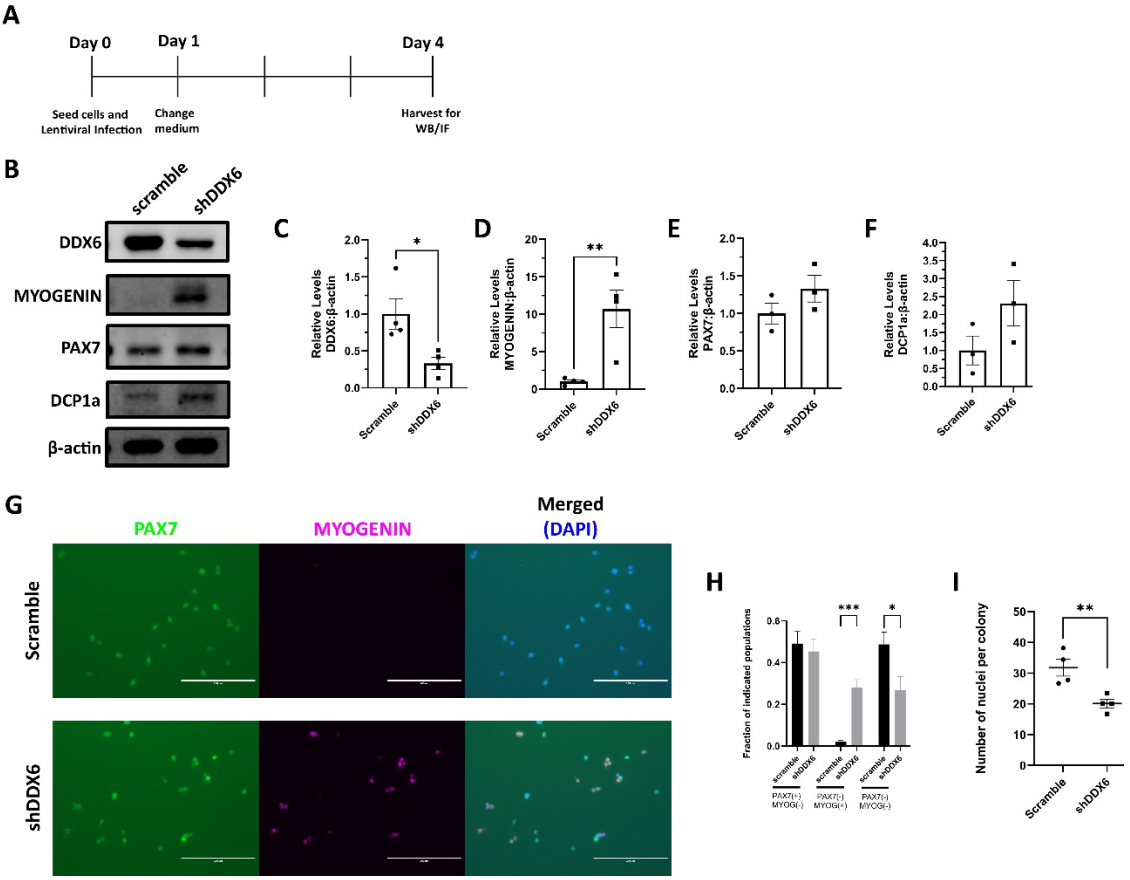

Figure 9. DDX6 knockdown pushes the satellite cells towards differentiation.

(A) Schematic illustration of the experiment.

(B) Immunoblotting of lysates with antibodies against DDX6, MYOG, PAX7, DCP1a and β-actin, after 4-day culture of satellite cells infected with scrambled shRNA and shRNA designed against DDX6 (shDDX6).

(C-F) Quantification of (C) DDX6, (D) MYOG, (E) PAX7, and (F) DCP1a in (B) by densitometry.

(G) Representative immunofluorescence analysis after 4-day culture of satellite cells infected with scrambled shRNA and shRNA designed against DDX6 (shDDX6).

(H) Quantification of fraction of indicated populations in (G).
(I) Quantification of number of nuclei per colony in (G).
Data are mean ±sem. *P<0.05, **P<0.01, ***P<0.001 (unpaired two-tailed Student's t-test), no significance unless specified. Scale bars: 200μm in G.

DDX6 has been reported to repress translation through mRNP granules (Di Stefano et al., 2019). To look at whether granules disassemble as the myogenic program proceeds, I stained MYOD to identify activated satellite cells in EDL myofiber after 48 and 72 hours of culture and look at the number of DDX6 granules. An insignificant decrease in the number of granules was observed from 48 hours to 72 hours of culture in MYOD expressing cells, with a p-vaule of 0.0743 (Figure 10A-B).

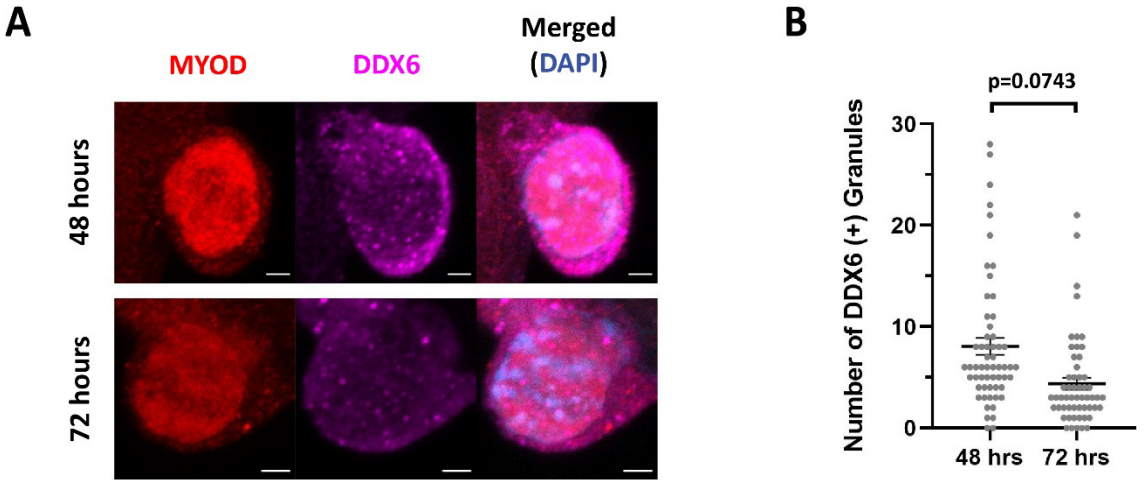

Figure 10. Number of DDX6 granules changes as the myogenic program proceeds.
(A) Representative immunofluorescence analysis of freshly isolated and cultured EDL myofiber from adult mice, with antibodies against MYOD (red) and DDX6 (purple). The upper panel is 48 hours, and the lower panel is 72 hours.
(B) Quantification of fraction of DDX6 (+) granules from (A).
Data are mean ±sem. *P<0.05, **P<0.01, ***P<0.001 (unpaired two-tailed Student's t-test), no significance unless specified. Scale bars: 2μm.

Chapter 4: Discussion

4.1 Knockout of TACC3 in quiescent satellite cells

Based on mass spectrometry and RNA-seq results in satellite cells cultured in sal003 versus DMSO (Fujita et al., 2021), *Tacc3* was chosen to be investigated in its role in satellite cell quiescence. Initially, *Tacc3* is hypothesized to be selectively translated in quiescent state based on the presence of uORFs and the increase in protein translation without an increase in RNA level in the presence of sal003 compared to DMSO control (Fujita et al., 2021). Other genes, such as Atf4, which also have uORFs, was shown to have higher protein levels in quiescent satellite cells compared to activated satellite cells, in agreement with the change in P-eIF2α level (Zismanov et al., 2016). However, here, TACC3 was found to be lowly expressed in quiescent satellite cells. The knockout of TACC3 in quiescent satellite cells further supports TACC3 may not have a role in maintaining quiescence (Figure 1). The knockout efficiency has been previously validated in muscle stem cells (Fujita et al., 2021). One of the possible explanations for the lack of phenotype may be *Tacc3* transcript level was low in quiescent satellite cells and the presence of uORFs in *Tacc3* transcripts is not enough to accumulate a high TACC3 protein level. By comparing the transcript level in quiescent satellite cells and activated satellite cells in publicly available RNA-seq data, *Tacc3* transcript level is indeed higher in activated satellite cells (Yue et al., 2020), in agreement with our immunostaining. The low *Tacc3* transcript level combined with low TACC3 protein level may explain the lack of observable phenotype on quiescent satellite cells.

Though the protein level of TACC3 was low in quiescent satellite cells, I tried to validate whether the knockout of TACC3 can still cause a shift in dynamic microtubule network to stable de-tyrosinated microtubule network without affecting the maintenance of quiescence. However, contrary to the initial hypothesis, de-tyrosinated microtubule network

was absent in both wild-type and TACC3 knockout quiescent satellite cells, suggesting TACC3 does not have a role in microtubules dynamics in quiescent satellite cells (Figure 2). The absence of the proposed phenotype may be due to the difference in cell type. Fibroblast also did not have a shift in microtubule dynamics when TACC3 was knocked down (Furey et al., 2020).

Though TACC3 does not have a role during quiescence, the level of TACC3 does increase in activated satellite cells (Figure 1) and a de-tyrosinated microtubule network was present in some activated satellite cells (data not shown). Since TACC3 regulates the microtubule nucleation during mitosis (Kinoshita et al., 2005), the upregulation in TACC3 during cell cycle re-entry to allow cell division may be reasonable. TACC3 was also shown to be important during muscle regeneration and self-renewal (Fujita et al., 2021). However, it remained unclear what is the exact function of TACC3 in activated satellite cells and why only some activated satellite cells have de-tyrosinated microtubule network. Interestingly, a subset of microtubules was found to be de-tyrosinated in epithelial cells and spatially concentrated with lysosomes to allow fusion with autophagosomes for the initiation of autophagy (Mohan et al., 2019). An increase in autophagy during activation was also reported in satellite cells (Tang and Rando, 2014). It may be interesting to further look at the role of de-tyrosinated microtubules in activated muscle stem cells.

4.2 Number of DDX6 granules during postnatal growth and myogenic program

Adult stem cells have tight translation regulation to maintain the proper stem cell function (Saba et al., 2021). In muscle stem cells, phosphorylation of translation initiation factor eIF2α is important in maintaining the quiescence of satellite cells (Zismanov et al., 2016). The activation of quiescent satellite cells is accompanied by the disassembly of mRNP granules (Crist et al., 2012) and dephosphorylation of eIF2α (Zismanov et al., 2016).

Considering the mRNP granules are directly correlated with the concentration of translationally repressed mRNPs (Franks and Lykke-Andersen, 2008), I hypothesized the mRNP granules will increase as the myogenic progenitors establish quiescence during postnatal growth. No significant change in the overall number of granules in myogenic progenitors was observed during postnatal growth (Figure 4). Therefore, no significant conclusion can be drawn. It may be due to heterogeneity between replicates. The myogenic progenitors during postnatal growth are composed of a mixture of proliferating cells and quiescent cells. To minimize the effect of heterogeneity, analyses were performed separately for PAX7(+) MYOD(+) and PAX7(+) MYOD(-) cells and a significant difference was indeed observed. Given during the establishment of quiescence, the PAX7(+) MYOD(+) cells need to downregulate MYOD, the difference in the number of granules between the PAX7(+) MYOD(+) cells and PAX7(+) MYOD(-) cells may indicate a requirement of decrease in the number of granules to downregulate MYOD or vice versa. However, the PAX7(+) MYOD(+) cells can be committed to either quiescence or differentiation, it, therefore, remains difficult to speculate what are the functions of the granules. One of the potential mechanisms may be the overall transcription and translation activities decrease as the cell enter quiescence. Since the formation of mRNP granules have been suggested to depend on the presence of mRNA (Garcia-Jove Navarro et al., 2019) and the concentration of the component on mRNP (Luo et al., 2018). Future studies will be required to further characterize the cells, such as their transcription and translation level to elucidate the potential mechanism for the change in the number of granules.

The data obtained have discrepancies with the initial hypothesis proposed. A higher number of granules was observed in PAX7(+) MYOD(+) cells during postnatal growth but disassembly of granules was reported during satellite cell activation (Crist et al., 2012). No significant decrease in the number of granules from 0 hour to 6 hours was observed, contrary

to previously reported data (Figure 6). Based on the correlation between the average intensity of PAX7 and the number of DDX6 granules (Figure 5), it is possible the discrepancy in observation was due to the satellite cells chosen during imaging. Through lineage tracing experiment using the tmx-inducible Cre mice to label cells which expressed PAX7 and immunostaining with PAX7, it was confirmed that the cells with low PAX7 staining are indeed PAX7 positive (data not shown). The consideration of these low PAX7 cells may be one of the reasons the number of granules was lower at 0 hour. Moreover, the discrepancy can also be observation bias. Between different researchers, the quantification parameters may vary and hence, a difference in the quantification outcome. For example, the reported average number of granules at 0 hour of culture varies in different studies, with an average of around 7 granules (Crist et al., 2012), around 40 granules (Kann et al., 2022), and around 5 granules in this study. In addition, it can also be contributed by the resolution of the microscope. Without a standardized quantification protocol, it remains unclear what is the implication of the difference in observation.

In addition, contrary to a decrease, a significant increase in the number of granules was observed from 6 hours to 24 hours. Since it was reported the majority of activated satellite cells (around 98%) express MYOD after 24 hours of culture (Zammit et al., 2002), the observation was similar to what was observed on postnatal day 28. To look closer into how the mRNP granules change, I focused on the granule type. It was reported that a higher number of granule structures, such as P-bodies, is observed in non-quiescent yeast cells (Lee et al., 2016). Moreover, the number of P-bodies fluctuates during cell cycle (Aizer et al., 2013). Perhaps suggesting the presence of granules in proliferating cells has some functional implications. I, therefore, checked the presence of P-bodies in quiescent and activated satellite cells. The fraction of DDX6 granules that are P-bodies is significantly higher in activated satellite cells compared to quiescent satellite cells, accompanied by stronger puncta

staining (Figure 7). Bioinformatics analysis using RNA-seq data for quiescent and activated satellite cells (Yue et al., 2020) was in agreement with the increase in DCP1a. A similar increase in P-bodies was also reported in a recent study (Roy et al., 2021). Given DCP1a is one of the top hit proteins in mass spectrometry data using DDX6 immunoprecipitation (Di Stefano et al., 2019), it is possible the increase in DDX6 granules may be caused by the increase in P-bodies through DCP1a upregulation. Further studies would be required to elucidate the function of P-bodies during activation. The result, however, may support the hypothesis that the granules undergo disassembly during activation. Since majority of the granules are DCP1a (-) during quiescence and DCP1a (+) during activation, it suggests the granule types are different and may have undergone disassembly during quiescence exit and assembly during the activation process. However, live cell imaging would be required to validate the granule dynamics. I, also, compared the fraction of DDX6 granules that are P-bodies in early postnatal growth (Figure 8). However, it remained similar to quiescent satellite cells, suggesting the myogenic progenitors in early postnatal may be different from the activated satellite cells. It may not be surprising given sc-RNA-seq has shown postnatal juvenile muscle stem cells are not equivalent to adult muscle stem cells (Xi et al., 2020). Though given the cells in postnatal timepoint were a mixture of proliferating and quiescent cells, it may not be a fair comparison. Although a similar observation of a higher fraction of P-bodies was seen in postnatal day 7 (data not shown), it may not be comparable since the digestion time used in postnatal day 7 was half of the one used in all other time points. The muscle sizes were too different to find a common digestion time as the time points used in this study. However, it may still imply there is functional importance of P-bodies in proliferating cells.

Here I reported the increase in P-bodies during activation. However, different mRNP components have been found in quiescent satellite cells, such as Staufen1 (de Morrée et al.,

2017) and FMRP (Crist et al., 2012; Fujita et al., 2017). It remains unknown whether the components in different granules are mutually exclusive and whether the function of the granule differs with composition. In mass spectrometry data for quiescent satellite cells versus activated satellite cells (Zheng et al., 2022), some components that are enriched in RNA granules, which was identified through FAPS of P-bodies (Hubstenberger et al., 2017), was found to be enriched in quiescent satellite cells or activated satellite cells (Figure S1). Some interesting examples include enrichment of HSPB1 in quiescent satellite cells, which has a function in anti-apoptosis (Katsogiannou et al., 2014) and localization to stress granules (Liu et al., 2020), and UPF1 in activated satellite cells, which is a core factor for nonsense-mediated mRNA decay (Park et al., 2020) and acts with STAUFEN1 to degrade MyoD transcript (de Morrée et al., 2017). It may provide a starting point to look closer into how the granule composition changes in the myogenic program. However, given the identification of the mRNP granules components were done in other cell types. It is crucial to identify what mRNP granules components are present in myogenic cells. Interestingly, both STAUFEN1 and FMRP granules are present in satellite cells but STAUFEN1 was reported to have low co-localization with DDX6 in satellite cells (de Morrée et al., 2017) while Staufen was reported to have co-localization with FMRP in human cells (Villacé et al., 2004). It is not known whether different cell types and different time points will affect the protein interaction. It is also implying the use of a single marker may not be able to conclude the overall number of mRNP granules.

4.3 Heterogeneity in quiescent satellite cells

Heterogeneity in satellite cells was indeed reported in several studies (Kuang et al., 2007; Rocheteau et al., 2012; Yartseva et al., 2020). Here I also observed a variable number of granules. Therefore, I ask if such variation was correlated with the quiescent state of adult satellite cells. Pearson correlation analysis showed a positive correlation between the PAX7

average fluorescence intensity and the number of granules (Figure 5). Interestingly, as the cells activate, the PAX7 level decreased, and the correlation was lost after 24 hours of culture. It may not be surprising since the majority of the granules became P-bodies after 24 hours of culture. The correlation between the number of granules may depend on granule type or the correlation was related to the quiescence of satellite cells. Whether PAX7 affects the number of granules would require overexpression and knockdown experiments to confirm its effect on the number of granules.

The heterogenous level of PAX7 observed in quiescent satellite cells may have two implications. First, the difference in PAX7 level indicates the cells are at different stages of activation. Indeed, the quiescent stem cells become activated as soon as the niche homeostasis is disrupted. Recent development in protocols to minimize transcriptional changes during tissue dissociation (Machado et al., 2021; Wu et al., 2017) have shown the rapid response in transcriptome during activation. *In vivo* fixation of quiescent satellite cells also showed the transcript level of PAX7 decreased during tissue digestion (Yue et al., 2020). It is possible the heterogeneity in quiescent satellite cells was a result of activation during digestion, which would be in agreement with the dissolution of granules to release *Myf5* transcript during activation (Crist et al., 2012). However, the myofiber digestion time was shorter and less damaging than the isolation protocol used in RNA-seq. It is not clear whether the protein level of PAX7 decreases drastically during the isolation of myofiber. Moreover, although we see a decrease in PAX7 after 6 hours of culture, the decrease was not significant, and some cells retained a high level of PAX7 and granules. *In vivo* fixation coupled with mass spectrometry or myofiber isolation will be required to confirm the hypothesis. The second implication of the data may be the satellite cells are truly heterogeneous. Given different studies have shown both the difference at the protein level and functional analysis of the subpopulations (Rocheteau et al., 2012; Der Vartanian et al., 2019; Scaramozza et al.,

2019), the difference in PAX7 and number of granules may reflect the intrinsic difference in satellite cells. The hypothesis of a kinetic model of mRNP granule formation suggests the number of granules is directly proportional to the translationally repressed mRNPs (Franks and Lykke-Andersen, 2008). The higher number of granules and PAX7 may coincide with the $PAX7^{High}$ population being more resistant to activation (Rocheteau et al., 2012) by preventing the release of repressed mRNP to form polysomes. Although it is not known whether the higher number of granules corresponds to a higher protein level of the components of mRNP granules, it may be interesting to compare the protein level by isolating the $PAX7^{High}$ and $PAX7^{Low}$ population or utilizing single-cell western blotting to verify the observation. Alternatively, a subpopulation that never expresses *Myf5* may potentially correspond to the $PAX7^{High}$ population given they both have a higher self-renewal (Kuang et al., 2007). It would provide an interesting model to see if these subpopulations indeed have higher translation repression through mRNP granules. It is also worth noting that the quantification of PAX7 protein intensity through immunofluorescence may be subjective. Further quantification through flow cytometry may give a more objective result. Moreover, with recent advance in flow cytometry, single cell analysis of protein intensity and subcellular localization became possible (Schraivogel et al., 2022). With further optimization in the staining protocol, it is possible to simultaneously obtain the PAX7 protein intensity and the number and localization of DDX6 (+) granules in single cell and perform cell sorting for downstream analysis.

4.4 Knockdown of DDX6 led to premature differentiation

A previous report in human myoblast (Di Stefano et al., 2019) showed an increase in differentiation when DDX6 is knockdown. I asked if it would have a similar effect in the freshly isolated satellite cells. Increase in differentiation marked by MYOGENIN and a decrease in cell number were observed, suggesting the cells have premature differentiation

(Figure 9). It was hypothesized the increase in differentiation was caused by the release of the transcript of a chromatin-remodeling enzyme *Kdm4b* targeting the gene Myogenin (Di Stefano et al., 2019). Depletion of KDM4B also showed a decrease in differentiation (Choi et al., 2015; Di Stefano et al., 2019), which may explain our observation in knockdown of DDX6 in satellite cells. In myofiber data, a decrease in granules with a p-value of 0.0743 was observed as the myogenic program proceeds, which may support the role of mRNP granules in the entrapment of transcripts such as *Kdm4b*. However, it is inconclusive whether the increase in differentiation was solely due to the disassembly of mRNP granules or DDX6. Further knockdown studies using other mRNP components may help to further elucidate the role of DDX6 and mRNP granules. Interestingly, the knockdown of DCP1a in myoblast led to hyperproliferation (Roy et al., 2021). Given the majority of DDX6 granules are also DCP1a positive, it may be worth checking whether knockdown of DCP1a affects the number of granules and increase the resistance to differentiation.

Chapter 5: Conclusions and Future Directions

In the first part of the thesis, I investigated the role of TACC3 during satellite cell quiescence. Contrary to the initial hypotheses, TACC3 did not have a role in the maintenance of quiescence and knockout of TACC3 in satellite cells did not shift the dynamic microtubule network to stable de-tyrosinated microtubule network.

In the second part of the thesis, I investigate whether there is a change in mRNP granules number and/or type during postnatal growth and myogenic program in adult satellite cells. Based on the myofiber data, I proposed a model (Figure 11) that when satellite cells activate, the number of P-bodies increases through upregulation of DCP1a. As the myogenic program proceeds, the number of mRNP granules decreases to allow differentiation.

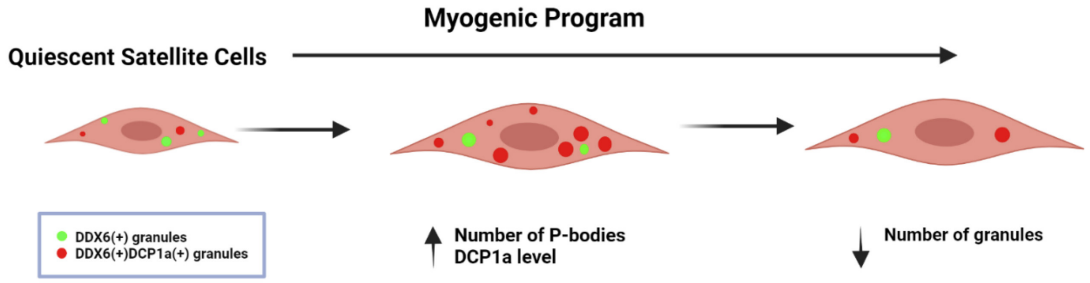

Figure 11. Proposed model for changes in mRNP granules in adult satellite cells during the myogenic program.

Although the data suggest the number of mRNP granules changes during the myogenic program, the process has never been shown through imaging in satellite cells. Several reports have been suggesting the mRNP granules are very dynamic, with rapid assembly and disassembly (Hofmann et al., 2021; Wheeler et al., 2016). However, the mRNP dynamics have never been studied in satellite cells. It is unknown whether this contributes to the heterogeneous number of granules observed in this study. The changes in granules may be a reflection of a shift in the steady-state in the assembly and disassembly of granules. It

would be interesting to generate a fusion protein of DDX6 and a fluorescent protein to study the dynamic of mRNP granules through live-cell imaging.

In addition, in the results, an increase in proportion of P-bodies during the myogenic program was observed. However, the interactome of DDX6 during different stages of myogenic program has not been addressed. Based on the proposed function of altering cytosolic concentration of the components of mRNP granule to mediate control over their functions (Hofmann et al., 2021), it will be interesting to further study this aspect through APEX mass spectrometry. Using bait proteins, such as DDX6 and DCP1a, to look at the interactome in different stages of myogenic program, it may reveal how the granules assemble and disassemble and reveal the compositions of the granules.

The challenge in the current study is a high heterogeneity is present, ranging from the difference in the initial quiescent state in satellite cells to cells at different stages in the myogenic program. Here, I showed in the quiescent state, the number of granules is correlated with the PAX7 level, which may contribute to the heterogeneity. The high heterogeneity may be the main contributor to no significance was found in the experiments. Variation in the average number of granules can be observed between replicates but a consistent correlation with PAX7 was also observed between replicates, suggesting the quantification is susceptible to observation bias. A high throughput analysis platform will be required to fully understand how the granules change during the myogenic program. Interestingly, such technology is beginning to emerge. A recent development in the FACS platform allows high-speed fluorescence image-enabled cell sorting, with the ability to record protein localization (Schraivogel et al., 2022). With a fluorescent protein tag in the DDX6 protein, such high throughput analysis may be possible alongside the functional analysis.

One major unresolved question in the study is whether the observation recapitulates the *in vivo* environment. One of the limitations of this study was the digestion process may affect the mRNP granules. In the study, the EDL muscle was digested in collagenase for 50 minutes, followed by trituration to obtain the single myofiber. Stress index was found to be positively correlated with dissociation time (Machado et al., 2021). Given stress induces the formation of mRNP granules, possibility that the digestion process had an effect on the number of granules observed cannot be ruled out. In addition, study through perfusion and tissue clearing showed a higher cell volume with long cell protrusions in quiescent satellite cells (Verma et al., 2018). In addition, without collagenase digestion, satellite cells in TA muscle also showed protrusions and branches in quiescent satellite cells (Ma et al., 2022). Yet, in the EDL myofiber data, though protrusions were sometimes observed, the length and morphology of the protrusions were not comparable to the reported observations. It is unknown how this impacts the mRNP granules. To rule out such possibility, *in vivo* fixation by paraformaldehyde perfusion may be a potential solution. Using *in vivo* fixation, the effect of digestion can be ruled out given the proteins will be fixed during the isolation process. It can better recapitulate the *in vivo* environment. Such method was utilized in the isolation of muscle stem cells for RNA-seq (van Velthoven et al., 2017; Yue et al., 2020). Development in a protocol to couple the *in vivo* fixation with the myofiber isolation will allow more insights in the study of mRNP granules. Alternatively, it is also possible to utilize the *in vivo* fixation with the protocol of isolating quiescent satellite cells to perform immunofluorescent analysis and confirm our observation. Moreover, this way, it is possible to perform muscle injury coupled with *in vivo* fixation to look at the changes in mRNP granules *in vivo*.

Another interesting approach to study the mRNP granules is to utilize the drug sal003. P-eIF2α was shown to be important in maintaining quiescence in satellite cells (Zismanov et al., 2016). Sal003, an inhibitor for eIF2α dephosphorylation (Robert et al., 2006), is able to

delay satellite cells activation and maintain low protein synthesis (Zismanov et al., 2016). With sal003, it is possible to ask whether the delay in satellite cells activation was accompanied by maintaining the mRNP granules and whether there would be an increase in P-bodies that occurred during activation. Moreover, combined with the knockdown of DDX6, it is possible to ask if the maintenance of PAX7 using sal003 requires DDX6. In addition, it may be possible to suggest what transcripts are sequestered by mRNP granules in a more quiescent state by treating the cells with sal003 and compare DDX6 knockdown with control. Based on quiescent versus activated satellite cells mass spectrometry data (Zheng et al., 2022) combined with RNA-seq data for mRNA enriched in mRNP granules (Hubstenberger et al., 2017) and RNA-seq data for satellite cells (Yue et al., 2020), it may provide some direction on what possible mRNA are targeted by mRNP granules (Figure S2). Transcripts for translation initiation, such as *Eif4a1*, and RNA surveillance, such as *Upf1*, are targeted by mRNP granules and upregulated in activated satellite cells without increase in RNA level (Figure S2). Further studies may give us more insights into the mechanism of translational control in satellite cells.

Lastly, given the current published data and the observed result, it would be interesting to generate DDX6 knockout mice to confirm the role of mRNP granules in maintaining quiescence. It is speculated the mRNP granules are important in sequestering the myogenic transcript during quiescence (Crist et al., 2012). However, there is not any direct evidence the mRNP granules are required. Several papers have been suggesting the structure of mRNP granules may not be required for translation repression (Chu and Rana, 2006, Eulalio et al., 2007). Currently, there is no study focusing on the role of mRNP granules in quiescence or postnatal growth. It would be interesting to generate knockout mice to investigate the role of DDX6 in entering and maintaining quiescence.

Chapter 6: Bibliography

Abdelhaleem, M., Maltais, L., & Wain, H. (2003). The human DDX and DHX gene families of putative RNA helicases. *Genomics, 81*(6), 618–622.

Adomavicius, T., Guaita, M., Zhou, Y., Jennings, M. D., Latif, Z., Roseman, A. M., & Pavitt, G. D. (2019). The structural basis of translational control by eIF2 phosphorylation. *Nature communications, 10*(1), 1-10.

Aizer, A., Brody, Y., Ler, L. W., Sonenberg, N., Singer, R. H., & Shav-Tal, Y. (2008). The dynamics of mammalian P body transport, assembly, and disassembly in vivo. *Molecular biology of the cell*, *19*(10), 4154–4166.

Aizer, A., Kafri, P., Kalo, A., & Shav-Tal, Y. (2013). The P body protein Dcp1a is hyper-phosphorylated during mitosis. *PloS one*, *8*(1), e49783.

Amorim, I. S., Lach, G., & Gkogkas, C. G. (2018). The Role of the Eukaryotic Translation Initiation Factor 4E (eIF4E) in Neuropsychiatric Disorders. *Frontiers in genetics, 9*, 561.

Ancel, S., Stuelsatz, P., & Feige, J. N. (2021). Muscle Stem Cell Quiescence: Controlling Stemness by Staying Asleep. *Trends in cell biology, 31*(7), 556–568.

Ayache, J., Bénard, M., Ernoult-Lange, M., Minshall, N., Standart, N., Kress, M., & Weil, D. (2015). P-body assembly requires DDX6 repression complexes rather than decay or Ataxin2/2L complexes. *Molecular biology of the cell*, *26*(14), 2579–2595.

Baghdadi, M. B., Castel, D., Machado, L., Fukada, S. I., Birk, D. E., Relaix, F., Tajbakhsh, S., & Mourikis, P. (2018). Reciprocal signalling by Notch-Collagen V-CALCR retains muscle stem cells in their niche. *Nature*, *557*(7707), 714–718.

Balachandran, S., & Barber, G. N. (2007). PKR in innate immunity, cancer, and viral oncolysis. *Methods in molecular biology (Clifton, N.J.), 383*, 277–301.

Balak, C., Bénard, M., Schaefer, E., Iqbal, S., Ramsey, K., Ernoult-Lange, M., ... & Piton, A. (2019). Rare de novo missense variants in RNA helicase DDX6 cause intellectual disability and dysmorphic features and lead to P-Body defects and RNA dysregulation. *The American Journal of Human Genetics*, *105*(3), 509-525.

Barruet, E., Garcia, S. M., Striedinger, K., Wu, J., Lee, S., Byrnes, L., Wong, A., Xuefeng, S., Tamaki, S., Brack, A. S., & Pomerantz, J. H. (2020). Functionally heterogeneous human satellite cells identified by single cell RNA sequencing. *eLife*, *9*, e51576.

Bi, P., McAnally, J. R., Shelton, J. M., Sánchez-Ortiz, E., Bassel-Duby, R., & Olson, E. N. (2018). Fusogenic micropeptide Myomixer is essential for satellite cell fusion and muscle regeneration. *Proceedings of the National Academy of Sciences of the United States of America*, *115*(15), 3864–3869.

Bjornson, C. R., Cheung, T. H., Liu, L., Tripathi, P. V., Steeper, K. M., & Rando, T. A. (2012). Notch signaling is necessary to maintain quiescence in adult muscle stem cells. *Stem cells (Dayton, Ohio)*, *30*(2), 232–242.

Brengues, M., Teixeira, D., & Parker, R. (2005). Movement of eukaryotic mRNAs between polysomes and cytoplasmic processing bodies. *Science (New York, N.Y.)*, *310*(5747), 486–489.

Bröhl, D., Vasyutina, E., Czajkowski, M. T., Griger, J., Rassek, C., Rahn, H. P., Purfürst, B., Wende, H., & Birchmeier, C. (2012). Colonization of the satellite cell niche by skeletal muscle progenitor cells depends on Notch signals. *Developmental cell*, *23*(3), 469–481.

Cai, D., McEwen, D. P., Martens, J. R., Meyhofer, E., & Verhey, K. J. (2009). Single molecule imaging reveals differences in microtubule track selection between Kinesin motors. *PLoS biology, 7*(10), e1000216.

Cairns J. (1975). Mutation selection and the natural history of cancer. *Nature*, *255*(5505), 197–200.

Carbonaro, M., O'Brate, A., & Giannakakou, P. (2011). Microtubule disruption targets HIF-1alpha mRNA to cytoplasmic P-bodies for translational repression. *The Journal of cell biology*, *192*(1), 83–99.

Castello, A., Fischer, B., Frese, C. K., Horos, R., Alleaume, A. M., Foehr, S., Curk, T., Krijgsveld, J., & Hentze, M. W. (2016). Comprehensive Identification of RNA-Binding Domains in Human Cells. *Molecular cell, 63*(4), 696–710.

Chen, W., Datzkiw, D., & Rudnicki, M. A. (2020). Satellite cells in ageing: use it or lose it. *Open biology, 10*(5), 200048.

Cheung, T. H., Quach, N. L., Charville, G. W., Liu, L., Park, L., Edalati, A., Yoo, B., Hoang, P., & Rando, T. A. (2012). Maintenance of muscle stem-cell quiescence by microRNA-489. *Nature*, *482*(7386), 524–528.

Choi, J. H., Song, Y. J., & Lee, H. (2015). The histone demethylase KDM4B interacts with MyoD to regulate myogenic differentiation in C2C12 myoblast cells. *Biochemical and biophysical research communications*, *456*(4), 872–878.

Choo, H. J., Canner, J. P., Vest, K. E., Thompson, Z., & Pavlath, G. K. (2017). A tale of two niches: differential functions for VCAM-1 in satellite cells under basal and injured conditions. *American journal of physiology. Cell physiology*, *313*(4), C392–C404.

Chu, C. Y., & Rana, T. M. (2006). Translation repression in human cells by microRNA-induced gene silencing requires RCK/p54. *PLoS biology*, *4*(7), e210.

Crist, C. G., Montarras, D., & Buckingham, M. (2012). Muscle satellite cells are primed for myogenesis but maintain quiescence with sequestration of Myf5 mRNA targeted by microRNA-31 in mRNP granules. *Cell stem cell*, *11*(1), 118–126.

Conboy, I. M., & Rando, T. A. (2002). The regulation of Notch signaling controls satellite cell activation and cell fate determination in postnatal myogenesis. *Developmental cell*, *3*(3), 397–409.

Coppin, L., Leclerc, J., Vincent, A., Porchet, N., & Pigny, P. (2018). Messenger RNA Life-Cycle in Cancer Cells: Emerging Role of Conventional and Non-Conventional RNA-Binding Proteins?. *International journal of molecular sciences, 19*(3), 650.

Courel, M., Clément, Y., Bossevain, C., Foretek, D., Vidal Cruchez, O., Yi, Z., Bénard, M., Benassy, M. N., Kress, M., Vindry, C., Ernoult-Lange, M., Antoniewski, C., Morillon, A., Brest, P., Hubstenberger, A., Roest Crollius, H., Standart, N., & Weil, D. (2019). GC content shapes mRNA storage and decay in human cells. *eLife*, *8*, e49708.

Cutler, A. A., Pawlikowski, B., Wheeler, J. R., Dalla Betta, N. C., Antwine, T., O'Rourke, R., ... & Olwin, B. B. (2021). The regenerating skeletal muscle niche guides muscle stem cell self-renewal. *bioRxiv*. https://doi.org/10.1101/635805

Dalla Costa, I., Buchanan, C. N., Zdradzinski, M. D., Sahoo, P. K., Smith, T. P., Thames, E., ... & Twiss, J. L. (2021). The functional organization of axonal mRNA transport and translation. *Nature Reviews Neuroscience*, *22*(2), 77-91.

de Morrée, A., van Velthoven, C., Gan, Q., Salvi, J. S., Klein, J., Akimenko, I., Quarta, M., Biressi, S., & Rando, T. A. (2017). Staufen1 inhibits MyoD translation to actively maintain muscle stem cell quiescence. *Proceedings of the National Academy of Sciences of the United States of America*, *114*(43), E8996–E9005.

de Valoir, T., Tucker, M. A., Belikoff, E. J., Camp, L. A., Bolduc, C., & Beckingham, K. (1991). A second maternally expressed Drosophila gene encodes a putative RNA helicase of the "DEAD box" family. *Proceedings of the National Academy of Sciences of the United States of America, 88*(6), 2113–2117.

de Vries, S., Naarmann-de Vries, I. S., Urlaub, H., Lue, H., Bernhagen, J., Ostareck, D. H., & Ostareck-Lederer, A. (2013). Identification of DEAD-box RNA helicase 6 (DDX6) as a cellular modulator of vascular endothelial growth factor expression under hypoxia. *The Journal of biological chemistry, 288*(8), 5815–5827.

Denes, L. T., Kelley, C. P., & Wang, E. T. (2021). Microtubule-based transport is essential to distribute RNA and nascent protein in skeletal muscle. *Nature communications, 12*(1), 6079.

Der Vartanian, A., Quétin, M., Michineau, S., Auradé, F., Hayashi, S., Dubois, C., Rocancourt, D., Drayton-Libotte, B., Szegedi, A., Buckingham, M., Conway, S. J., Gervais, M., & Relaix, F. (2019). PAX3 Confers Functional Heterogeneity in Skeletal Muscle Stem Cell Responses to Environmental Stress. *Cell stem cell, 24*(6), 958–973.e9.

Di Stefano, B., Luo, E. C., Haggerty, C., Aigner, S., Charlton, J., Brumbaugh, J., Ji, F., Rabano Jiménez, I., Clowers, K. J., Huebner, A. J., Clement, K., Lipchina, I., de Kort, M., Anselmo, A., Pulice, J., Gerli, M., Gu, H., Gygi, S. P., Sadreyev, R. I., Meissner, A., … Hochedlinger, K. (2019). The RNA Helicase DDX6 Controls Cellular Plasticity by Modulating P-Body Homeostasis. *Cell stem cell, 25*(5), 622–638.e13.

Döhla, J., Kuuluvainen, E., Gebert, N., Amaral, A., Englund, J. I., Gopalakrishnan, S., ... & Katajisto, P. (2022). Metabolic determination of cell fate through selective inheritance of mitochondria. *Nature Cell Biology, 24*(2), 148-154.

Donnelly, N., Gorman, A. M., Gupta, S., & Samali, A. (2013). The eIF2α kinases: their structures and functions. *Cellular and molecular life sciences : CMLS*, *70*(19), 3493–3511.

Dumont, N. A., Wang, Y. X., Von Maltzahn, J., Pasut, A., Bentzinger, C. F., Brun, C. E., & Rudnicki, M. A. (2015). Dystrophin expression in muscle stem cells regulates their polarity and asymmetric division. *Nature medicine, 21*(12), 1455-1463.

Eliazer, S., Muncie, J. M., Christensen, J., Sun, X., D'Urso, R. S., Weaver, V. M., & Brack, A. S. (2019). Wnt4 from the Niche Controls the Mechano-Properties and Quiescent State of Muscle Stem Cells. *Cell stem cell*, *25*(5), 654–665.e4.

Eulalio, A., Behm-Ansmant, I., Schweizer, D., & Izaurralde, E. (2007). P-body formation is a consequence, not the cause, of RNA-mediated gene silencing. *Molecular and cellular biology*, *27*(11), 3970–3981.

Evano, B., Khalilian, S., Le Carrou, G., Almouzni, G., & Tajbakhsh, S. (2020). Dynamics of Asymmetric and Symmetric Divisions of Muscle Stem Cells In Vivo and on Artificial Niches. *Cell reports*, *30*(10), 3195–3206.e7.

Eystathioy, T., Chan, E. K., Tenenbaum, S. A., Keene, J. D., Griffith, K., & Fritzler, M. J. (2002). A phosphorylated cytoplasmic autoantigen, GW182, associates with a unique population of human mRNAs within novel cytoplasmic speckles. *Molecular biology of the cell*, *13*(4), 1338–1351.

Feige, P., Brun, C. E., Ritso, M., & Rudnicki, M. A. (2018). Orienting Muscle Stem Cells for Regeneration in Homeostasis, Aging, and Disease. *Cell stem cell*, *23*(5), 653–664.

Fujita, R., Jamet, S., Lean, G., Cheng, H. C. M., Hébert, S., Kleinman, C. L., & Crist, C. (2021). Satellite cell expansion is mediated by P-eIF2α-dependent Tacc3 translation. *Development, 148*(2), dev194480.

Fujita, R., Zismanov, V., Jacob, J. M., Jamet, S., Asiev, K., & Crist, C. (2017). Fragile X mental retardation protein regulates skeletal muscle stem cell activity by regulating the stability of Myf5 mRNA. *Skeletal muscle*, *7*(1), 18.

Furey, C., Jovasevic, V., & Walsh, D. (2020). TACC3 Regulates Microtubule Plus-End Dynamics and Cargo Transport in Interphase Cells. *Cell reports*, *30*(1), 269–283.e6.

Garcia-Jove Navarro, M., Kashida, S., Chouaib, R., Souquere, S., Pierron, G., Weil, D., & Gueroui, Z. (2019). RNA is a critical element for the sizing and the composition of phase-separated RNA-protein condensates. *Nature communications*, *10*(1), 3230.

García-Prat, L., Perdiguero, E., Alonso-Martín, S., Dell'Orso, S., Ravichandran, S., Brooks, S. R., Juan, A. H., Campanario, S., Jiang, K., Hong, X., Ortet, L., Ruiz-Bonilla, V., Flández, M., Moiseeva, V., Rebollo, E., Jardí, M., Sun, H. W., Musarò, A., Sandri, M., Del Sol, A., … Muñoz-Cánoves, P. (2020). FoxO maintains a genuine muscle stem-cell quiescent state until geriatric age. *Nature cell biology, 22*(11), 1307–1318.

Gayraud-Morel, B., Chrétien, F., Jory, A., Sambasivan, R., Negroni, E., Flamant, P., Soubigou, G., Coppée, J. Y., Di Santo, J., Cumano, A., Mouly, V., & Tajbakhsh, S. (2012). Myf5 haploinsufficiency reveals distinct cell fate potentials for adult skeletal muscle stem cells. *Journal of cell science*, *125*(Pt 7), 1738–1749.

Gattazzo, F., Laurent, B., Relaix, F., Rouard, H., & Didier, N. (2020). Distinct Phases of Postnatal Skeletal Muscle Growth Govern the Progressive Establishment of Muscle Stem Cell Quiescence. *Stem cell reports*, *15*(3), 597–611.

Goel, A. J., Rieder, M. K., Arnold, H. H., Radice, G. L., & Krauss, R. S. (2017). Niche Cadherins Control the Quiescence-to-Activation Transition in Muscle Stem Cells. *Cell reports, 21*(8), 2236–2250.

Gorbalenya, A. E., & Koonin, E. V. (1993). Helicases: amino acid sequence comparisons and structure-function relationships. *Current opinion in structural biology*, *3*(3), 419-429.

Han, T. W., Kato, M., Xie, S., Wu, L. C., Mirzaei, H., Pei, J., Chen, M., Xie, Y., Allen, J., Xiao, G., & McKnight, S. L. (2012). Cell-free formation of RNA granules: bound RNAs identify features and components of cellular assemblies. *Cell*, *149*(4), 768–779.

Hentze, M. W., Castello, A., Schwarzl, T., & Preiss, T. (2018). A brave new world of RNA-binding proteins. *Nature reviews. Molecular cell biology, 19*(5), 327–341.

Hofmann, S., Kedersha, N., Anderson, P., & Ivanov, P. (2021). Molecular mechanisms of stress granule assembly and disassembly. *Biochimica et Biophysica Acta (BBA)-Molecular Cell Research*, *1868*(1), 118876.

Horvathova, I., Voigt, F., Kotrys, A. V., Zhan, Y., Artus-Revel, C. G., Eglinger, J., Stadler, M. B., Giorgetti, L., & Chao, J. A. (2017). The Dynamics of mRNA Turnover Revealed by Single-Molecule Imaging in Single Cells. *Molecular cell*, *68*(3), 615–625.e9.

Hubstenberger, A., Courel, M., Bénard, M., Souquere, S., Ernoult-Lange, M., Chouaib, R., Yi, Z., Morlot, J. B., Munier, A., Fradet, M., Daunesse, M., Bertrand, E., Pierron, G., Mozziconacci, J., Kress, M., & Weil, D. (2017). P-Body Purification Reveals the Condensation of Repressed mRNA Regulons. *Molecular cell*, *68*(1), 144–157.e5.

Judson, R. N., Tremblay, A. M., Knopp, P., White, R. B., Urcia, R., De Bari, C., Zammit, P. S., Camargo, F. D., & Wackerhage, H. (2012). The Hippo pathway member Yap plays a key role in influencing fate decisions in muscle satellite cells. *Journal of cell science*, *125*(Pt 24), 6009–6019.

Kann, A. P., Hung, M., Wang, W., Nguyen, J., Gilbert, P. M., Wu, Z., & Krauss, R. S. (2022). An injury-responsive Rac-to-Rho GTPase switch drives activation of muscle stem cells through rapid cytoskeletal remodeling. *Cell stem cell, 29*(6), 933–947.e6.

Kato, M., Han, T. W., Xie, S., Shi, K., Du, X., Wu, L. C., Mirzaei, H., Goldsmith, E. J., Longgood, J., Pei, J., Grishin, N. V., Frantz, D. E., Schneider, J. W., Chen, S., Li, L., Sawaya, M. R., Eisenberg, D., Tycko, R., & McKnight, S. L. (2012). Cell-free formation of RNA granules: low complexity sequence domains form dynamic fibers within hydrogels. *Cell*, *149*(4), 753–767.

Katsogiannou, M., Andrieu, C., & Rocchi, P. (2014). Heat shock protein 27 phosphorylation state is associated with cancer progression. *Frontiers in genetics, 5*, 346.

Kedersha, N. L., Gupta, M., Li, W., Miller, I., & Anderson, P. (1999). RNA-binding proteins TIA-1 and TIAR link the phosphorylation of eIF-2 alpha to the assembly of mammalian stress granules. *The Journal of cell biology*, *147*(7), 1431–1442.

Kedersha, N., Cho, M. R., Li, W., Yacono, P. W., Chen, S., Gilks, N., Golan, D. E., & Anderson, P. (2000). Dynamic shuttling of TIA-1 accompanies the recruitment of mRNA to mammalian stress granules. *The Journal of cell biology*, *151*(6), 1257–1268.

Kedersha, N., Panas, M. D., Achorn, C. A., Lyons, S., Tisdale, S., Hickman, T., Thomas, M., Lieberman, J., McInerney, G. M., Ivanov, P., & Anderson, P. (2016). G3BP-Caprin1-USP10 complexes mediate stress granule condensation and associate with 40S subunits. *The Journal of cell biology*, *212*(7), 845–860.

Kimball, S. R., Horetsky, R. L., Ron, D., Jefferson, L. S., & Harding, H. P. (2003). Mammalian stress granules represent sites of accumulation of stalled translation initiation complexes. *American journal of physiology. Cell physiology*, *284*(2), C273–C284.

Kinoshita, K., Noetzel, T. L., Pelletier, L., Mechtler, K., Drechsel, D. N., Schwager, A., ... & Hyman, A. A. (2005). Aurora A phosphorylation of TACC3/maskin is required for centrosome-dependent microtubule assembly in mitosis. *The Journal of cell biology*, *170*(7), 1047-1055.

Koromilas A. E. (2019). M(en)TORship lessons on life and death by the integrated stress response. *Biochimica et biophysica acta. General subjects, 1863*(3), 644–649.

Kuang, S., Kuroda, K., Le Grand, F., & Rudnicki, M. A. (2007). Asymmetric self-renewal and commitment of satellite stem cells in muscle. *Cell*, *129*(5), 999–1010.

LaBarge, M. A., & Blau, H. M. (2014). Skeletal Muscle Stem Cells. In *Essentials of Stem Cell Biology* (pp. 267-279). Academic Press.

Ladomery, M., Wade, E., & Sommerville, J. (1997). Xp54, the Xenopus homologue of human RNA helicase p54, is an integral component of stored mRNP particles in oocytes. *Nucleic acids research*, *25*(5), 965–973.

Lagord, C., Soulet, L., Bonavaud, S., Bassaglia, Y., Rey, C., Barlovatz-Meimon, G., Gautron, J., & Martelly, I. (1998). Differential myogenicity of satellite cells isolated from extensor digitorum longus (EDL) and soleus rat muscles revealed in vitro. *Cell and tissue research*, *291*(3), 455–468.

Lai, A., Valdez-Sinon, A. N., & Bassell, G. J. (2020). Regulation of RNA granules by FMRP and implications for neurological diseases. *Traffic (Copenhagen, Denmark)*, *21*(7), 454–462.

Lee, H. Y., Cheng, K. Y., Chao, J. C., & Leu, J. Y. (2016). Differentiated cytoplasmic granule formation in quiescent and non-quiescent cells upon chronological aging. *Microbial cell (Graz, Austria)*, *3*(3), 109–119.

Linder, P., Lasko, P. F., Ashburner, M., Leroy, P., Nielsen, P. J., Nishi, K., Schnier, J., & Slonimski, P. P. (1989). Birth of the D-E-A-D box. *Nature*, *337*(6203), 121–122.

Linder, P., & Jankowsky, E. (2011). From unwinding to clamping - the DEAD box RNA helicase family. *Nature reviews. Molecular cell biology*, *12*(8), 505–516.

Lindsay, A. J., & McCaffrey, M. W. (2011). Myosin Va is required for P body but not stress granule formation. *The Journal of biological chemistry*, *286*(13), 11519–11528.

Liu, J., Rivas, F. V., Wohlschlegel, J., Yates, J. R., 3rd, Parker, R., & Hannon, G. J. (2005a). A role for the P-body component GW182 in microRNA function. *Nature cell biology*, *7*(12), 1261–1266.

Liu, J., Valencia-Sanchez, M. A., Hannon, G. J., & Parker, R. (2005b). MicroRNA-dependent localization of targeted mRNAs to mammalian P-bodies. *Nature cell biology, 7*(7), 719–723.

Liu, Z., Zhang, S., Gu, J., Tong, Y., Li, Y., Gui, X., Long, H., Wang, C., Zhao, C., Lu, J., He, L., Li, Y., Liu, Z., Li, D., & Liu, C. (2020). Hsp27 chaperones FUS phase separation under the modulation of stress-induced phosphorylation. *Nature structural & molecular biology, 27*(4), 363–372.

Lukjanenko, L., Karaz, S., Stuelsatz, P., Gurriaran-Rodriguez, U., Michaud, J., Dammone, G., Sizzano, F., Mashinchian, O., Ancel, S., Migliavacca, E., Liot, S., Jacot, G., Metairon, S., Raymond, F., Descombes, P., Palini, A., Chazaud, B., Rudnicki, M. A., Bentzinger, C. F., & Feige, J. N. (2019). Aging Disrupts Muscle Stem Cell Function by Impairing Matricellular WISP1 Secretion from Fibro-Adipogenic Progenitors. *Cell stem cell*, *24*(3), 433–446.e7.

Lumb, J. H., Li, Q., Popov, L. M., Ding, S., Keith, M. T., Merrill, B. D., Greenberg, H. B., Li, J. B., & Carette, J. E. (2017). DDX6 Represses Aberrant Activation of Interferon-Stimulated Genes. *Cell reports*, *20*(4), 819–831.

Luo, Y., Na, Z., & Slavoff, S. A. (2018). P-Bodies: Composition, Properties, and Functions. *Biochemistry*, *57*(17), 2424–2431.

Loschi, M., Leishman, C. C., Berardone, N., & Boccaccio, G. L. (2009). Dynein and kinesin regulate stress-granule and P-body dynamics. *Journal of cell science*, *122*(Pt 21), 3973–3982.

Ma, N., Chen, D., Lee, J. H., Kuri, P., Hernandez, E. B., Kocan, J., Mahmood, H., Tichy, E. D., Rompolas, P., & Mourkioti, F. (2022). Piezo1 regulates the regenerative capacity of skeletal muscles via orchestration of stem cell morphological states. *Science advances, 8*(11), eabn0485.

Machado, L., Geara, P., Camps, J., Dos Santos, M., Teixeira-Clerc, F., Van Herck, J., Varet, H., Legendre, R., Pawlotsky, J. M., Sampaolesi, M., Voet, T., Maire, P., Relaix, F., & Mourikis, P. (2021). Tissue damage induces a conserved stress response that initiates quiescent muscle stem cell activation. *Cell stem cell*, *28*(6), 1125–1135.e7.

Madisen, L., Zwingman, T. A., Sunkin, S. M., Oh, S. W., Zariwala, H. A., Gu, H., ... & Zeng, H. (2010). A robust and high-throughput Cre reporting and characterization system for the whole mouse brain. *Nature neuroscience*, *13*(1), 133-140.

Magiera, M. M., & Janke, C. (2014). Post-translational modifications of tubulin. *Current biology : CB*, *24*(9), R351–R354.

Marmor-Kollet, H., Siany, A., Kedersha, N., Knafo, N., Rivkin, N., Danino, Y. M., Moens, T. G., Olender, T., Sheban, D., Cohen, N., Dadosh, T., Addadi, Y., Ravid, R., Eitan, C., Toth Cohen, B., Hofmann, S., Riggs, C. L., Advani, V. M., Higginbottom, A., Cooper-Knock, J., … Hornstein, E. (2020). Spatiotemporal Proteomic Analysis of Stress Granule Disassembly Using APEX Reveals Regulation by SUMOylation and Links to ALS Pathogenesis. *Molecular cell*, *80*(5), 876–891.e6.

Massenet, J., Gardner, E., Chazaud, B., & Dilworth, F. J. (2021). Epigenetic regulation of satellite cell fate during skeletal muscle regeneration. *Skeletal Muscle, 11*(1), 1-16.

Mateju, D., Eichenberger, B., Voigt, F., Eglinger, J., Roth, G., & Chao, J. A. (2020). Single-Molecule Imaging Reveals Translation of mRNAs Localized to Stress Granules. *Cell*, *183*(7), 1801–1812.e13.

Mauro, A. (1961). Satellite cell of skeletal muscle fibers. *The Journal of biophysical and biochemical cytology*, *9*(2), 493–495.

Millay, D. P., Sutherland, L. B., Bassel-Duby, R., & Olson, E. N. (2014). Myomaker is essential for muscle regeneration. *Genes & development*, *28*(15), 1641-1646.

Mohan, N., Sorokina, E. M., Verdeny, I. V., Alvarez, A. S., & Lakadamyali, M. (2019). Detyrosinated microtubules spatially constrain lysosomes facilitating lysosome–autophagosome fusion. *Journal of Cell Biology*, *218*(2), 632-643.

Montarras, D., Morgan, J., Collins, C., Relaix, F., Zaffran, S., Cumano, A., Partridge, T., & Buckingham, M. (2005). Direct isolation of satellite cells for skeletal muscle regeneration. *Science (New York, N.Y.)*, *309*(5743), 2064–2067.

Moss, F. P., & Leblond, C. P. (1970). Nature of dividing nuclei in skeletal muscle of growing rats. *The Journal of cell biology*, *44*(2), 459–462.

Mourikis, P., Sambasivan, R., Castel, D., Rocheteau, P., Bizzarro, V., & Tajbakhsh, S. (2012). A critical requirement for notch signaling in maintenance of the quiescent skeletal muscle stem cell state. *Stem cells (Dayton, Ohio)*, *30*(2), 243–252.

Muddashetty RS, Nalavadi VC, Gross C, et al. Reversible inhibition of PSD-95 mRNA translation by miR-125a, FMRP phosphorylation, and mGluR signaling. *Mol Cell*. 2011;42(5):673-688.

Murphy, M. M., Lawson, J. A., Mathew, S. J., Hutcheson, D. A., & Kardon, G. (2011). Satellite cells, connective tissue fibroblasts and their interactions are crucial for muscle regeneration. *Development*, *138*(17), 3625-3637.

Nadezhdina, E. S., Lomakin, A. J., Shpilman, A. A., Chudinova, E. M., & Ivanov, P. A. (2010). Microtubules govern stress granule mobility and dynamics. *Biochimica et biophysica acta*, *1803*(3), 361–371.

Nielsen, K. H., Chamieh, H., Andersen, C. B., Fredslund, F., Hamborg, K., Le Hir, H., & Andersen, G. R. (2009). Mechanism of ATP turnover inhibition in the EJC. *RNA (New York, N.Y.)*, *15*(1), 67–75.

O'Brien, J., Hayder, H., Zayed, Y., & Peng, C. (2018). Overview of microRNA biogenesis, mechanisms of actions, and circulation. *Frontiers in endocrinology, 9*, 402.

Olguin, H. C., & Olwin, B. B. (2004). Pax-7 up-regulation inhibits myogenesis and cell cycle progression in satellite cells: a potential mechanism for self-renewal. *Developmental biology*, *275*(2), 375–388.

Ono, Y., Boldrin, L., Knopp, P., Morgan, J. E., & Zammit, P. S. (2010). Muscle satellite cells are a functionally heterogeneous population in both somite-derived and branchiomeric muscles. *Developmental biology*, *337*(1), 29–41.

Pager, C. T., Schütz, S., Abraham, T. M., Luo, G., & Sarnow, P. (2013). Modulation of hepatitis C virus RNA abundance and virus release by dispersion of processing bodies and enrichment of stress granules. *Virology, 435*(2), 472–484.

Park, Y., Park, J., Hwang, H. J., Kim, B., Jeong, K., Chang, J., ... & Kim, Y. K. (2020). Nonsense-mediated mRNA decay factor UPF1 promotes aggresome formation. *Nature communications, 11*(1), 1-15.

Parker, R., & Sheth, U. (2007). P bodies and the control of mRNA translation and degradation. *Molecular cell, 25*(5), 635–646.

Rajgor, D., & Shanahan, C. M. (2014). RNA granules and cytoskeletal links. *Biochemical Society transactions*, *42*(4), 1206–1210.

Reineke, L. C., & Neilson, J. R. (2019). Differences between acute and chronic stress granules, and how these differences may impact function in human disease. *Biochemical pharmacology*, *162*, 123–131.

Relaix, F., Bencze, M., Borok, M. J., Der Vartanian, A., Gattazzo, F., Mademtzoglou, D., ... & Rotini, A. (2021). Perspectives on skeletal muscle stem cells. *Nature Communications, 12*(1), 1-11.

Relaix, F., Montarras, D., Zaffran, S., Gayraud-Morel, B., Rocancourt, D., Tajbakhsh, S., Mansouri, A., Cumano, A., & Buckingham, M. (2006). Pax3 and Pax7 have distinct and overlapping functions in adult muscle progenitor cells. *The Journal of cell biology*, *172*(1), 91–102.

Reznik M. (1969). Thymidine-3H uptake by satellite cells of regenerating skeletal muscle. *The Journal of cell biology*, *40*(2), 568–571.

Robert, F., Kapp, L. D., Khan, S. N., Acker, M. G., Kolitz, S., Kazemi, S., Kaufman, R. J., Merrick, W. C., Koromilas, A. E., Lorsch, J. R., & Pelletier, J. (2006). Initiation of protein synthesis by hepatitis C virus is refractory to reduced eIF2.GTP.Met-tRNA(i)(Met) ternary complex availability. *Molecular biology of the cell*, *17*(11), 4632–4644.

Rocheteau, P., Gayraud-Morel, B., Siegl-Cachedenier, I., Blasco, M. A., & Tajbakhsh, S. (2012). A subpopulation of adult skeletal muscle stem cells retains all template DNA strands after cell division. *Cell*, *148*(1-2), 112–125.

Rodgers, J. T., King, K. Y., Brett, J. O., Cromie, M. J., Charville, G. W., Maguire, K. K., Brunson, C., Mastey, N., Liu, L., Tsai, C. R., Goodell, M. A., & Rando, T. A. (2014). mTORC1 controls the adaptive transition of quiescent stem cells from G0 to G(Alert). *Nature*, *510*(7505), 393–396.

Roy, N., Sundar, S., Pillai, M., Patell-Socha, F., Ganesh, S., Aloysius, A., Rumman, M., Gala, H., Hughes, S. M., Zammit, P. S., & Dhawan, J. (2021). mRNP granule proteins Fmrp and Dcp1a differentially regulate mRNP complexes to contribute to control of muscle stem cell quiescence and activation. *Skeletal muscle*, *11*(1), 18.

Saba, J. A., Liakath-Ali, K., Green, R., & Watt, F. M. (2021). Translational control of stem cell function. *Nature Reviews Molecular Cell Biology*, *22*(10), 671-690.

Scaramozza, A., Park, D., Kollu, S., Beerman, I., Sun, X., Rossi, D. J., Lin, C. P., Scadden, D. T., Crist, C., & Brack, A. S. (2019). Lineage Tracing Reveals a Subset of Reserve Muscle Stem Cells Capable of Clonal Expansion under Stress. *Cell stem cell*, *24*(6), 944–957.e5.

Schmalbruch, H. (1976). The morphology of regeneration of skeletal muscles in the rat. *Tissue and Cell*, *8*(4), 673-692.

Schraivogel, D., Kuhn, T. M., Rauscher, B., Rodríguez-Martínez, M., Paulsen, M., Owsley, K., Middlebrook, A., Tischer, C., Ramasz, B., Ordoñez-Rueda, D., Dees, M., Cuylen-Haering, S., Diebold, E., & Steinmetz, L. M. (2022). High-speed fluorescence image-enabled cell sorting. *Science (New York, N.Y.)*, *375*(6578), 315–320.

Schultz E. (1996). Satellite cell proliferative compartments in growing skeletal muscles. *Developmental biology*, *175*(1), 84–94.

Seale, P., Sabourin, L. A., Girgis-Gabardo, A., Mansouri, A., Gruss, P., & Rudnicki, M. A. (2000). Pax7 is required for the specification of myogenic satellite cells. *Cell*, *102*(6), 777–786.

Sen, G. L., & Blau, H. M. (2005). Argonaute 2/RISC resides in sites of mammalian mRNA decay known as cytoplasmic bodies. *Nature cell biology*, *7*(6), 633–636.

Serman, A., Le Roy, F., Aigueperse, C., Kress, M., Dautry, F., & Weil, D. (2007). GW body disassembly triggered by siRNAs independently of their silencing activity. *Nucleic acids research*, *35*(14), 4715-4727.

Shah, K. H., Nostramo, R., Zhang, B., Varia, S. N., Klett, B. M., & Herman, P. K. (2014). Protein kinases are associated with multiple, distinct cytoplasmic granules in quiescent yeast cells. *Genetics*, *198*(4), 1495–1512.

Shang, M., Cappellesso, F., Amorim, R., Serneels, J., Virga, F., Eelen, G., Carobbio, S., Rincon, M. Y., Maechler, P., De Bock, K., Ho, P. C., Sandri, M., Ghesquière, B., Carmeliet, P., Di Matteo, M., Berardi, E., & Mazzone, M. (2020). Macrophage-derived glutamine boosts satellite cells and muscle regeneration. *Nature*, *587*(7835), 626–631.

Sheth, U., & Parker, R. (2003). Decapping and decay of messenger RNA occur in cytoplasmic processing bodies. *Science (New York, N.Y.)*, *300*(5620), 805–808.

Siegel, A. L., Kuhlmann, P. K., & Cornelison, D. D. (2011). Muscle satellite cell proliferation and association: new insights from myofiber time-lapse imaging. *Skeletal muscle*, *1*(1), 7.

Singh, G., Pratt, G., Yeo, G. W., & Moore, M. J. (2015). The Clothes Make the mRNA: Past and Present Trends in mRNP Fashion. *Annual review of biochemistry*, *84*, 325–354.

Strahl-Bolsinger, S., & Tanner, W. (1993). A yeast gene encoding a putative RNA helicase of the "DEAD"-box family. *Yeast (Chichester, England)*, *9*(4), 429–432.

Tang, A. H., & Rando, T. A. (2014). Induction of autophagy supports the bioenergetic demands of quiescent muscle stem cell activation. *The EMBO journal*, *33*(23), 2782–2797.

Teixeira, D., Sheth, U., Valencia-Sanchez, M. A., Brengues, M., & Parker, R. (2005). Processing bodies require RNA for assembly and contain nontranslating mRNAs. *RNA (New York, N.Y.)*, *11*(4), 371–382.

Thomas, M. G., Martinez Tosar, L. J., Desbats, M. A., Leishman, C. C., & Boccaccio, G. L. (2009). Mammalian Staufen 1 is recruited to stress granules and impairs their assembly. *Journal of cell science, 122*(Pt 4), 563–573.

Tian, S., Curnutte, H. A., & Trcek, T. (2020). RNA Granules: A View from the RNA Perspective. *Molecules (Basel, Switzerland)*, *25*(14), 3130.

Tierney, M. T., Gromova, A., Sesillo, F. B., Sala, D., Spenlé, C., Orend, G., & Sacco, A. (2016). Autonomous extracellular matrix remodeling controls a progressive adaptation in muscle stem cell regenerative capacity during development. *Cell reports*, *14*(8), 1940-1952.

Troy, A., Cadwallader, A. B., Fedorov, Y., Tyner, K., Tanaka, K. K., & Olwin, B. B. (2012). Coordination of satellite cell activation and self-renewal by Par-complex-dependent asymmetric activation of p38α/β MAPK. *Cell stem cell*, *11*(4), 541–553.

van Velthoven, C., de Morree, A., Egner, I. M., Brett, J. O., & Rando, T. A. (2017). Transcriptional Profiling of Quiescent Muscle Stem Cells In Vivo. *Cell reports*, *21*(7), 1994–2004.

Verma, M., Asakura, Y., Murakonda, B., Pengo, T., Latroche, C., Chazaud, B., McLoon, L. K., & Asakura, A. (2018). Muscle Satellite Cell Cross-Talk with a Vascular Niche Maintains Quiescence via VEGF and Notch Signaling. *Cell stem cell, 23*(4), 530–543.e9.

Villacé, P., Marión, R. M., & Ortín, J. (2004). The composition of Staufen-containing RNA granules from human cells indicates their role in the regulated transport and translation of messenger RNAs. *Nucleic acids research*, *32*(8), 2411–2420.

Walker, J. E., Saraste, M., Runswick, M. J., & Gay, N. J. (1982). Distantly related sequences in the alpha- and beta-subunits of ATP synthase, myosin, kinases and other ATP-requiring enzymes and a common nucleotide binding fold. *The EMBO journal*, *1*(8), 945–951.

Wang, J., Choi, J. M., Holehouse, A. S., Lee, H. O., Zhang, X., Jahnel, M., Maharana, S., Lemaitre, R., Pozniakovsky, A., Drechsel, D., Poser, I., Pappu, R. V., Alberti, S., & Hyman, A. A. (2018). A Molecular Grammar Governing the Driving Forces for Phase Separation of Prion-like RNA Binding Proteins. *Cell*, *174*(3), 688–699.e16.

Wang, Y., Arribas-Layton, M., Chen, Y., Lykke-Andersen, J., & Sen, G. L. (2015). DDX6 Orchestrates Mammalian Progenitor Function through the mRNA Degradation and Translation Pathways. *Molecular cell*, *60*(1), 118–130.

Weston, A., & Sommerville, J. (2006). Xp54 and related (DDX6-like) RNA helicases: roles in messenger RNP assembly, translation regulation and RNA degradation. *Nucleic acids research*, *34*(10), 3082–3094.

Wheeler, J. R., Matheny, T., Jain, S., Abrisch, R., & Parker, R. (2016). Distinct stages in stress granule assembly and disassembly. *eLife*, *5*, e18413.

Wen, Y., Bi, P., Liu, W., Asakura, A., Keller, C., & Kuang, S. (2012). Constitutive Notch activation upregulates Pax7 and promotes the self-renewal of skeletal muscle satellite cells. *Molecular and cellular biology, 32*(12), 2300–2311.

Wolf, N., Priess, J., & Hirsh, D. (1983). Segregation of germline granules in early embryos of Caenorhabditis elegans: an electron microscopic analysis. *Journal of embryology and experimental morphology*, *73*, 297–306.

Wu, Y. E., Pan, L., Zuo, Y., Li, X., & Hong, W. (2017). Detecting activated cell populations using single-cell RNA-seq. *Neuron*, *96*(2), 313-329.

Xi, H., Langerman, J., Sabri, S., Chien, P., Young, C. S., Younesi, S., Hicks, M., Gonzalez, K., Fujiwara, W., Marzi, J., Liebscher, S., Spencer, M., Van Handel, B., Evseenko, D., Schenke-Layland, K., Plath, K., & Pyle, A. D. (2020). A Human Skeletal Muscle Atlas Identifies the Trajectories of Stem and Progenitor Cells across Development and from Human Pluripotent Stem Cells. *Cell stem cell, 27*(1), 158–176.e10.

Yang, Q., Del Campo, M., Lambowitz, A. M., & Jankowsky, E. (2007). DEAD-box proteins unwind duplexes by local strand separation. *Molecular cell*, *28*(2), 253–263.

Yang, Q., & Jankowsky, E. (2005). ATP-and ADP-dependent modulation of RNA unwinding and strand annealing activities by the DEAD-box protein DED1. *Biochemistry*, *44*(41), 13591-13601.

Yao, R., Oyanagi, J., Natsume, Y., Kusama, D., Kato, Y., Nagayama, S., & Noda, T. (2016). Suppression of intestinal tumors by targeting the mitotic spindle of intestinal stem cells. *Oncogene*, *35*(47), 6109-6119.

Yartseva, V., Goldstein, L. D., Rodman, J., Kates, L., Chen, M. Z., Chen, Y. J., Foreman, O., Siebel, C. W., Modrusan, Z., Peterson, A. S., & Jovičić, A. (2020). Heterogeneity of Satellite Cells Implicates DELTA1/NOTCH2 Signaling in Self-Renewal. *Cell reports*, *30*(5), 1491–1503.e6.

Yennek, S., Burute, M., Théry, M., & Tajbakhsh, S. (2014). Cell adhesion geometry regulates non-random DNA segregation and asymmetric cell fates in mouse skeletal muscle stem cells. *Cell reports*, *7*(4), 961–970.

Yue, L., Wan, R., Luan, S., Zeng, W., & Cheung, T. H. (2020). Dek modulates global intron retention during muscle stem cells quiescence exit. *Developmental cell*, *53*(6), 661-676.

Yue, F., Oprescu, S. N., Qiu, J., Gu, L., Zhang, L., Chen, J., ... & Kuang, S. (2022). Lipid droplet dynamics regulate adult muscle stem cell fate. *Cell reports*, *38*(3), 110267.

Zammit, P. S., Golding, J. P., Nagata, Y., Hudon, V., Partridge, T. A., & Beauchamp, J. R. (2004). Muscle satellite cells adopt divergent fates: a mechanism for self-renewal?. *The Journal of cell biology*, *166*(3), 347-357.

Zammit, P. S., Heslop, L., Hudon, V., Rosenblatt, J. D., Tajbakhsh, S., Buckingham, M. E., Beauchamp, J. R., & Partridge, T. A. (2002). Kinetics of myoblast proliferation show that resident satellite cells are competent to fully regenerate skeletal muscle fibers. *Experimental cell research*, *281*(1), 39–49.

Zeng, W., Yue, L., Lam, K.S.W., Zhang, W., So, W.K., Tse, E.H.Y., & Cheung T.H. (2022). CPEB1 directs muscle stem cell activation by reprogramming the translational landscape. *Nature communications, 13*(947).

Zhang, L., Noguchi, Y. T., Nakayama, H., Kaji, T., Tsujikawa, K., Ikemoto-Uezumi, M., Uezumi, A., Okada, Y., Doi, T., Watanabe, S., Braun, T., Fujio, Y., & Fukada, S. I. (2019). The CalcR-PKA-Yap1 Axis Is Critical for Maintaining Quiescence in Muscle Stem Cells. *Cell reports, 29*(8), 2154–2163.e5.

Zheng, J. T., Lin, C. X., Fang, Z. Y., & Li, H. D. (2020). Intron Retention as a Mode for RNA-Seq Data Analysis. *Frontiers in genetics, 11*, 586.

Zhou, S., Han, L., & Wu, Z. (2022). A Long Journey before Cycling: Regulation of Quiescence Exit in Adult Muscle Satellite Cells. *International journal of molecular sciences, 23*(3), 1748.

Zismanov, V., Chichkov, V., Colangelo, V., Jamet, S., Wang, S., Syme, A., ... & Crist, C. (2016). Phosphorylation of eIF2α is a translational control mechanism regulating muscle stem cell quiescence and self-renewal. *Cell stem cell*, *18*(1), 79-90.

Appendices

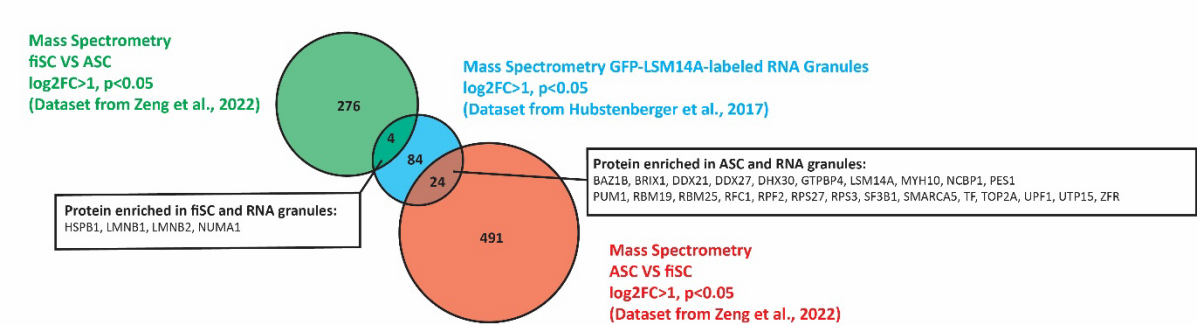

Figure S1. Venn diagram for protein enriched in freshly isolated satellite cells (fiSC) and activated satellite cells (ASC) and RNA granules. Proteins significantly enriched in mass spectrometry data for fiSC versus ASC (Zheng et al., 2022). Proteins significantly enriched in mass spectrometry data data for GFP-LSM14A labelled RNA granules isolated through FAPS (Hubstenberger et al., 2017)

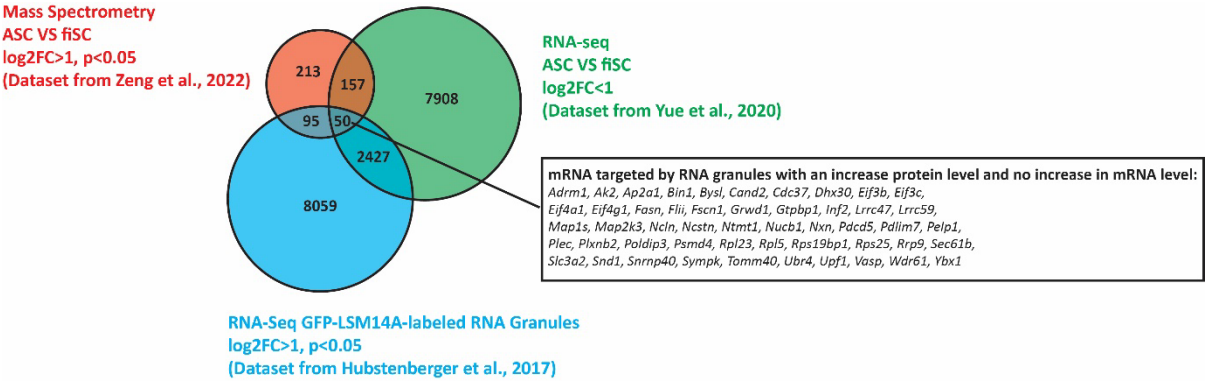

Figure S2. Venn diagram for mRNA targeted by RNA granules and proteins enriched in activated satellite cells (ASC) compared to freshly isolated satellites cells (fiSC) without increase in RNA level. Proteins significantly enriched in ASC compared to fiSC in mass spectrometry data for fiSC (Zheng et al., 2022). mRNA that has no increase in transcript level in RNA-seq data in ASC versus fiSC (Yue et al., 2020). mRNA significantly enriched in RNA-seq data for GFP-LSM14A labelled RNA granules isolated through FAPS (Hubstenberger et al., 2017).